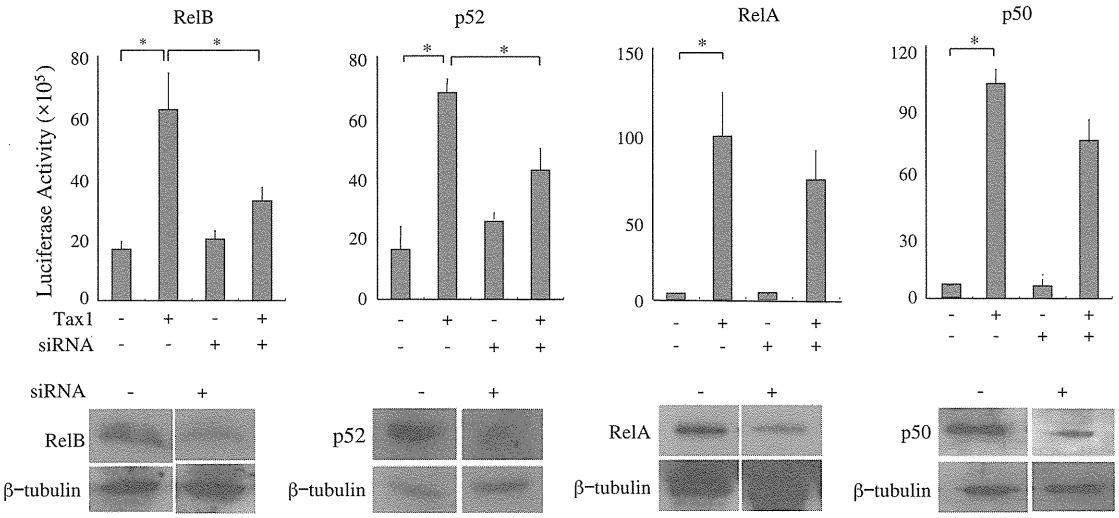

Fig. 3. Effects of siRNA for RelB, p52, RelA and p50 on κB site activation. REF52 cells were transfected with siRNA (10 nM) for RelB, p52, RelA and p50, and, one day after, introduced with pIgκB-Luc with or without pMT-2Tax in Lipofectamine 2000. Cells were harvested for luciferase activity determination 24 h after transfection with the reporter plasmid. Luciferase activity was normalized to protein content. Data are means ± SE. $^{*}P < 0.05$. Western blotting with antibodies to RelB, p52, RelA, p50 and β-tubulin was performed with lysates from cells transfected with siRNA.

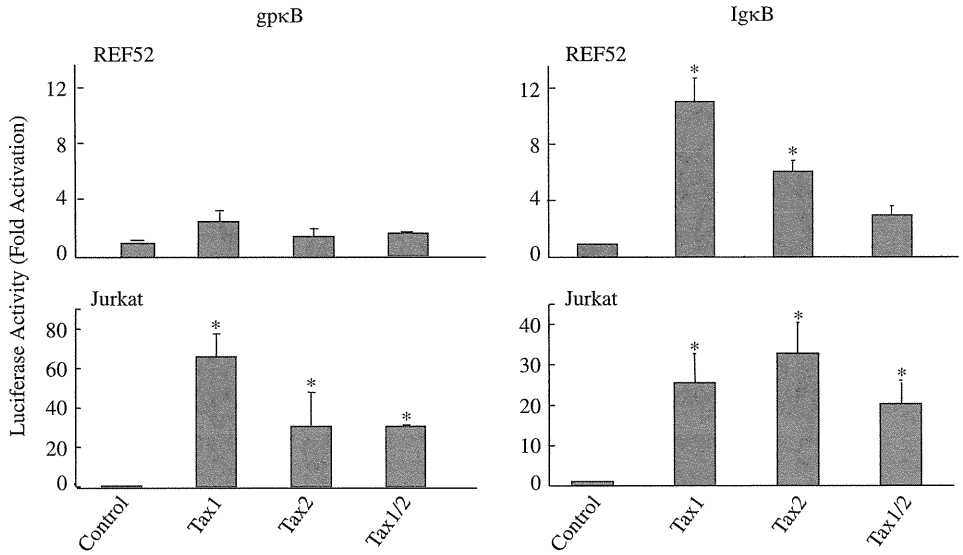

Fig. 4. Effects of Tax2 on gpκB site activation. REF52 and Jurkat cells were transfected with Tax1, Tax2 or Tax1/2 expression plasmid along with the gpκB or IgκB reporter plasmid and pCMV-β-gal. Cells were cultured for 48 h and harvested for luciferase activity determination. Luciferase activity was normalized to β-galactosidase activity. Data are means ± SE. $^{*}P < 0.05$.

formed with the gpκB site when nuclear extracts were prepared from Tax1-expressing REF52 cells (Fig. S2).

Immunofluorescence staining confirmed the results of EMSA. Tax1 introduction did not appreciably alter localization of RelA predominantly localized in the cytoplasm in those cells except for HeLa cells (Fig. 5A, C and D). In HeLa cells after Tax1 transfection, RelA was seen in the nucleus as well as the cytoplasm irrespective of Tax1 expression. This RelA expression might be attributable to Tax1-dependent paracrine mechanism, because HeLa cells even without Tax1 expression expressed RelA in the nucleus as indicated by arrowheads in Fig. 5D. The p50 molecule was mainly seen in the peri-nuclear region. RelB was present in the cytoplasm before introduction of Tax1 like RelA. In contrast to RelA, Tax1 facilitated the influx of RelB to the nucleus. Immunostaining with anti-p52 antibody detected p100/p52 mainly in the cytoplasm without Tax1 and in both the cytoplasm and nucleus with Tax1. Western blot examination also showed that RelB and p52 were seen in the nucleus after Tax1 was expressed, while RelA stayed in the cytoplasm even after Tax1 introduction in REF52 and MG63 cells (Fig. 5E and G). HeLa cells showed RelA translocation to the nucleus, as discussed before (Fig. 5H). In contrast, Jurkat cells exhibited translocation of RelA, as well as RelB and p52, in a Tax1-dependent manner (Fig. 5B and F).

RelA and p50 expressed in REF52 cells were examined for their function by stimulation with tumor necrosis factor α (TNFα). TNFα induced activation of the IgκB site in the luciferase reporter assays in association with translocation of RelA from the cytoplasm to the nucleus and phosphorylation of IκBα potentially leading to degradation (Fig. 5I–K). MG63 and HeLa cells also showed TNFα-induced RelA translocation (Fig. 5G and H). These

results suggest that RelA/p50 is functional in those non-hematopoietic cell lines.

Tax1 induces RelB and p52 binding to the IgκB site in vivo

In order to examine the ability of the IgκB site to bind NF-κB subunits in cells, we performed the chromatin immunoprecipitation (ChIP) assays in REF52, MG63 and HeLa cells with or without Tax1 expression (Fig. 7A, C and D). After reporter plasmid transfection with or without the Tax1 expression plasmid, cells were lysed and immunoprecipitated by anti-NF-κB subunit antibodies. None of the antibodies used precipitated appreciable gpκB and IgκB site DNA elements without Tax1 expression (Fig. 7A). Immunoprecipitation with anti-RelB, anti-p52 and anti-p50 antibodies detected the IgκB site with Tax1 expression. In addition, HeLa cells showed RelA binding to the IgκB site (Fig. 7D). As expected, only anti-p50 antibody precipitated the gpκB site in REF52 cells with Tax1 expression. Antibodies to RelA, RelB and p52 did not effectively precipitate the gpκB site in REF52 cells. These results indicate that at least REF52 and MG63 cells do not have the active form of the RelA/p50 complex in the nucleus in the presence of Tax1. In Jurkat cells, both the gpκB and IgκB sites were immunoprecipitated with all antibodies used in a Tax1-dependent manner (Fig. 7B).

Discussion

The present study demonstrates that the gpκB site is activated by HTLV-1 Tax1 in a cell type-dependent manner. Hematopoietic cell lines Jurkat, Raji and K562 activated the gpκB site upon Tax1 expression, whereas the seven non-hematopoietic cell lines failed to activate the gpκB site. One the other hand, the IgκB site was activated by Tax1 in both hematopoietic and non-hematopoietic cell lines used in this study. As overexpression of the canonical pathway subunit RelA activated the gpκB in non-hematopoietic cells, the gpκB unresponsiveness is presumably due to inactivation of the NF-κB canonical pathway by Tax1 in those cell lines. These results also suggest that the gpκB site is probably activated by the canonical pathway, but not by the non-canonical pathway, in the non-hematopoietic cell lines. Many NF-κB binding sites have been identified, most of which are activated by the canonical and non-canonical pathways. The gpκB site may be a unique case of NF-κB responsive elements that may discriminate the canonical pathway from the non-canonical pathway. Among three transcription factor pathways, involving NF-κB, CREB and SRF, which are directly activated by Tax1, Tax1-mediated NF-κB activation has been studied extensively and intensively. This is because ATL cells, including their derivative cell lines, carry constitutively active NF-κB (Yoshida et al., 1982). Studies suggest a close link between

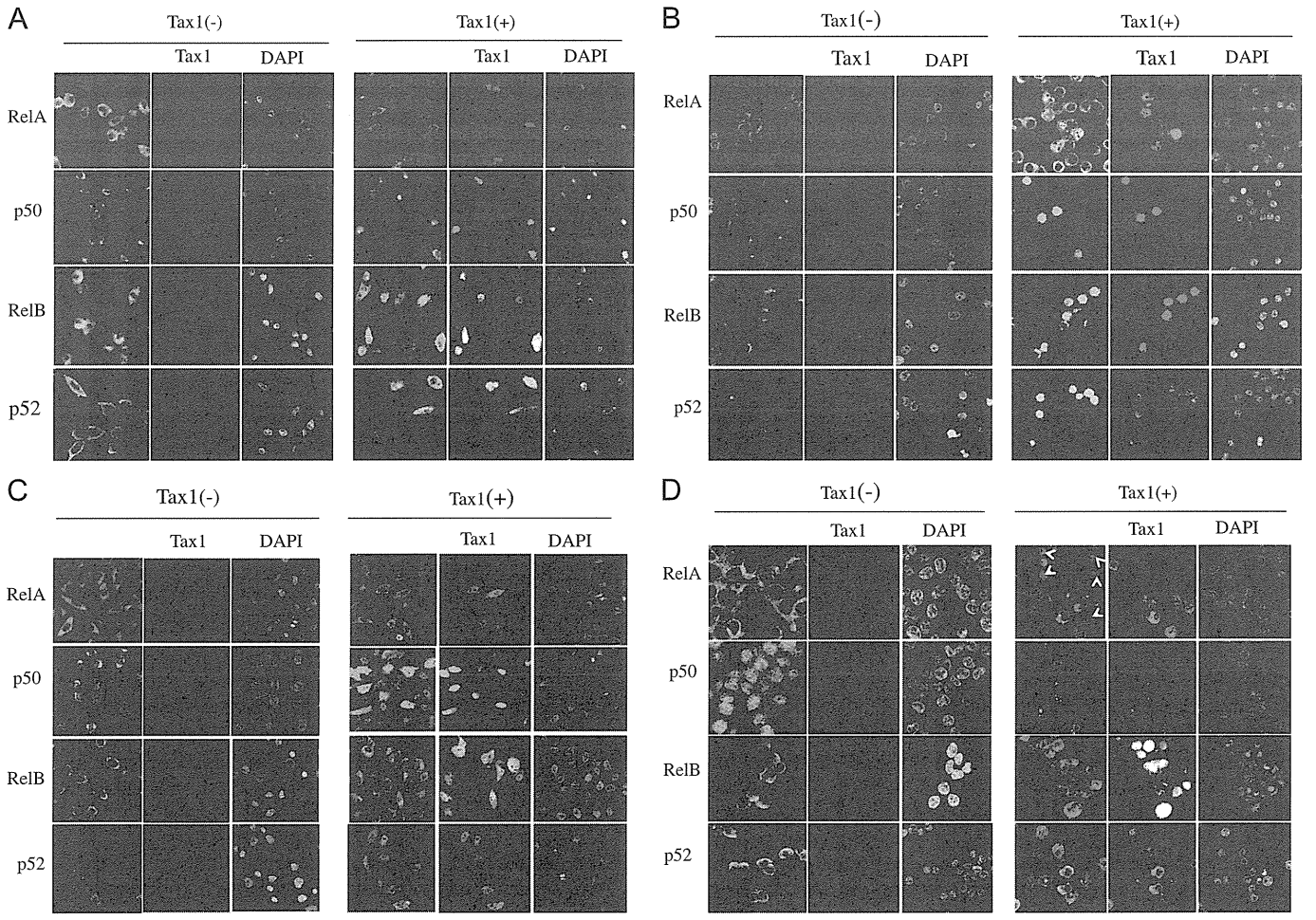

Fig. 5. Expression and function of NF-κB subunits. REF52 (A), Jurkat (B), MG63 (C) and HeLa (D) cells were transfected with or without pMT-2Tax, permealized, stained with the indicated antibodies and observed under a confocal microscope. DAPI was used for nuclear staining. Arrowheads indicate HeLa cells which express RelA in the nucleus without Tax1 expression. For Western blotting, lysates were prepared from REF52 (E) and Jurkat (F) transfected with pMT-2Tax, and MG63 (G) and HeLa (H) cells transfected with pMT-2Tax or cultured with TNFα, electrophoresed and transferred onto membranes. The membranes were treated by ECL system with the indicated antibodies. C23 and β-tubulin were used as marker proteins in nucleic and cytoplasmic fractions, respectively. REF52 cells were cultured with TNFα and examined for IgκB site responses in luciferase reporter assays (I), IκBα phosphorylation in Western blotting (K) and RelA and RelB localization in immunostaining (J). Data are means ± SE. $^{*}P < 0.05$.

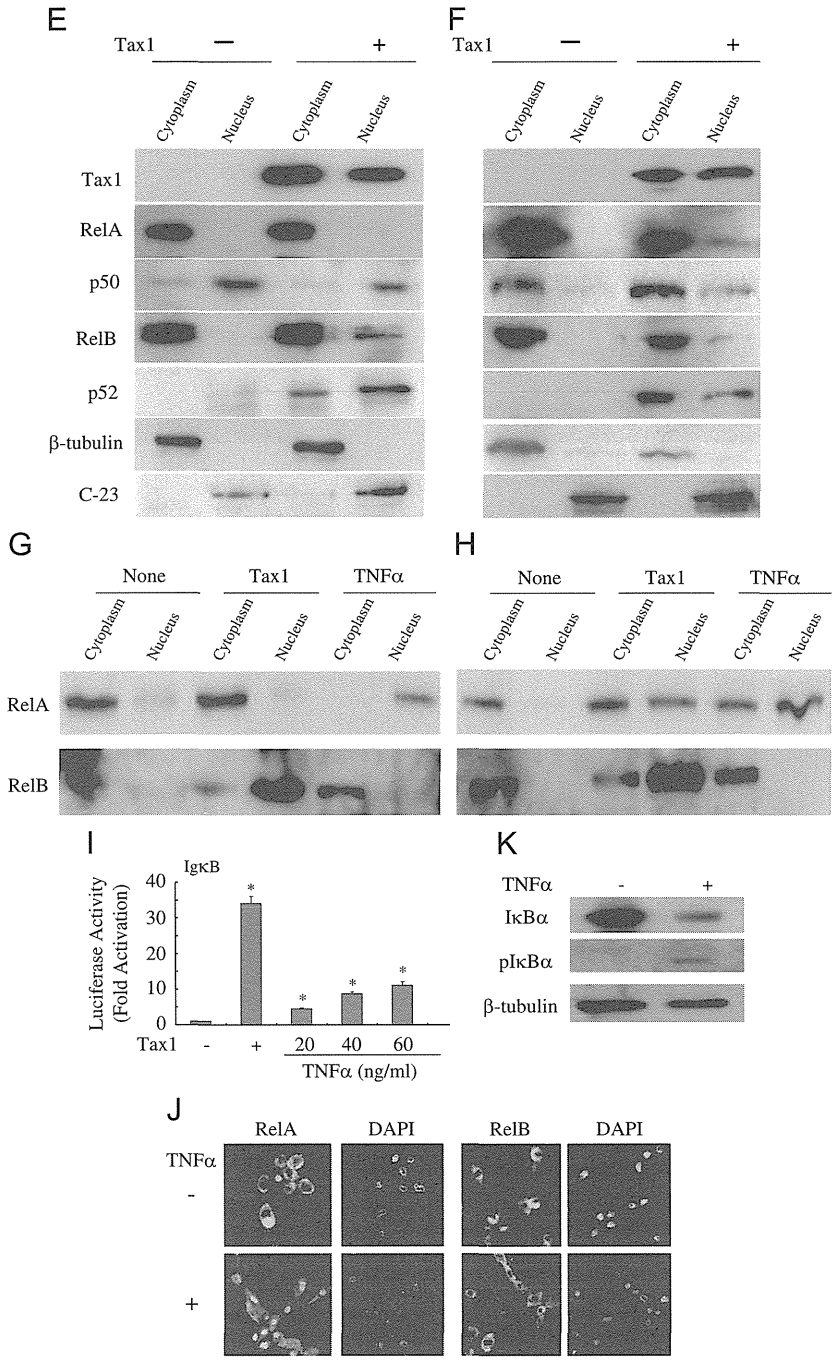

Fig. 5. (*continued*)

Tax1 and malignant transformation (Grossman et al., 1995; Matsuoka and Jeang, 2007; Shoji et al., 2009). In fact, Tax1 mutants lacking the ability to activate NF-κB show poor transforming activity. HTLV-2 Tax2 activates NF-κB similar to Tax1, however malignant transformation by Tax2 has rarely been reported (Higuchi and Fujii, 2009).

In contrast to Tax1, Tax2 immortalizes primary T cells efficiently (our unpublished observations). The efficient immortalization by Tax2 may be attributed to Tax2 specific effects such as activation of nuclear factor of activaed T cells (NF-AT) (Niinuma et al., 2005). We previously demonstrated that Tax1 scarcely induces production of IL-2 in T cells (Mizuguchi et al., 2009). Our results in this study exhibited different activation patterns of the NF-κB binding sites by Tax1 and Tax2; for example, Tax2 activated the IgκB site less extensively than Tax1 in REF52 cells (Fig. 4). Taking account of the poor ability of Tax2 to activate the non-canonical pathway, this is somewhat unexpected. The difference may be a result that NF-AT is activated by Tax2 but not by either Tax1 or Tax1/2, and also the IgκB site may be responsive to NF-AT. Similarly, in Jurkat cells, gpκB response to Tax2 was less than that to Tax1 (Fig. 4). Tax1 activates the canonical and non-canonical pathways in Jurkat cells, inducing full activation of NF-κB. Tax2 and Tax1/2 predominantly activate the canonical pathway, presumably resulting in reduced response of the gpκB site to Tax2, compared with response to Tax1. The different effects of Tax1 and Tax2 on activation of the κB sites may be closely associated with the differences in pathogenesis by infection with HTLV-1 and HTLV-2.

These assumptions may raise the question why the gpκB site is not capable of binding of RelB and p52 in non-hematopoietic cell

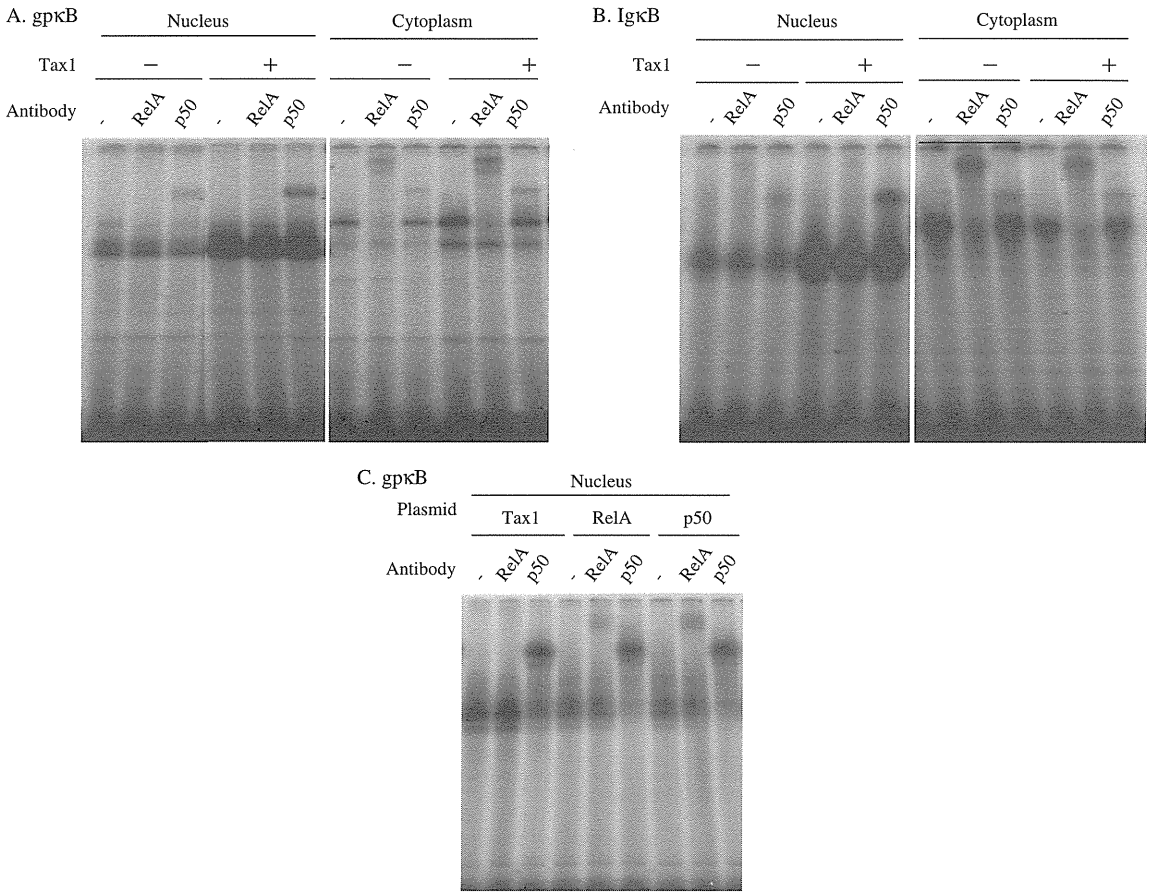

Fig. 6. NF-κB binding to κB sites *in vitro*. The gpκB (A and C) and IgκB (B) sites were used as probes. Probes were labeled and incubated with either nuclear extracts or cytoplasmic extracts prepared from REF52 cells with or without Tax1 expression. Antibodies for RelA and p50 were added to the reaction mixture 1 h prior to the addition of probes. Samples were electrophoresed on polyacrylamide gels and autoradiographed.

lines. It is obvious that Tax1-expressing those cells contained active non-canonical complex RelB/p52, because the IgκB site recruited the RelB/p52 complex (Fig. 7A). However the gpκB site did not show appreciable binding of RelB and p52. At this moment, a solid answer to this question has not been found. Association of RelB and p52 with the gpκB site may be dependent on RelA and p50 binding to the site. This notion may be supported by the result that all four subunits of NF-κB are associated with the gpκB site in Tax1-expressing Jurkat cells (Fig. 7B). Further examination is necessary to clarify this issue.

To gain insight into the mechanism accounting for inactivation of the canonical pathway in non-hematopoietic cell lines, we examined the expression of the canonical pathway subunits RelA and p50. Both molecules were expressed in REF52 cells at a protein level. Although p50 was present in the nucleus and able to bind the gpκB site upon Tax1 expression, RelA was not found in the nucleus even after Tax1 introduction (Figs. 5 and 7). EMSA examination demonstrated complex formation of RelA and p50 with the gpκB site using cytoplasmic lysates, suggesting that the functional complex of RelA and p50 is present in REF52 cells. The gpκB site is capable of RelA/p50 binding. Since Tax1 has been shown to activate the RelA and p50 complex by interaction with IKKγ in the IKK complex (Harhaj et al., 1999; Jin et al., 1999b), we further examined expression of IKKγ by immunostaining with anti-IKKγ antibody. Our observations clearly showed that IKKγ was present in REF52 cells (data not shown). These results imply that an unknown mechanism inhibiting the activation of the canonical pathway complex RelA and p50 may be present in non-hematopoietic cell lines. This mechanism might be related to the process of translocation from the cytoplasm to the nucleus, because RelA was not seen in the nucleus in Tax1 expressing cells.

Cell type-dependent activation of NF-κB by Tax1 is reminiscent of Tax1-mediated activation of the transcription factor E2F. Tax1 activated E2F in hematopoietic cells, however REF52 cells showed little effect of Tax1 on E2F function (Ohtani et al., 2000). Although a cellular factor mediating Tax1-dependent activation of E2F is not known, the Tax1 mutant without the ability to activate NF-κB is also unable to activate E2F (Ohtani et al., 2000). In addition, we observed that Tax2 lacked the ability to activate E2F (our unpublished results). E2F plays critical roles, as a transcription factor, in cell proliferation through progression of the G1 to S phase transition in the cell cycle (Mizuguchi et al., 2011; Ohtani and Nakamura, 2002). Collectively, development of cell transformation by Tax1 may require activation of both the canonical and non-canonical pathways, which are not associated with non-hematopoietic cell lines and Tax2, respectively.

In summary, HTLV-1 Tax1 does not activate the canonical NF-κB pathway in the non-hematopoietic cell lines used in this study and the NF-κB binding site in the OX40L promoter does not respond to the non-canonical pathway in those cells.

Materials and methods

Cell culture

REF52, MG63, HeLa and 293T cells were cultured in Dulbecco's modified Eagle's medium (DMEM) supplemented with 10% fetal

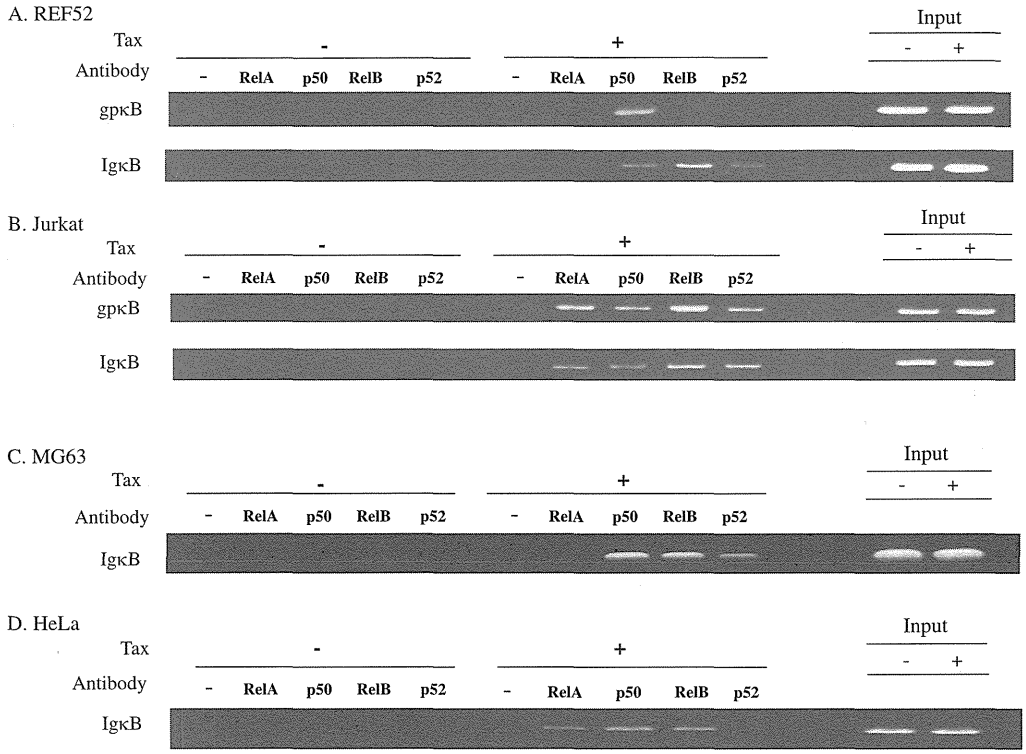

Fig. 7. NF-κB binding to κB sites *in vivo*. Chromatin complexes were prepared from REF52 (A), Jurkat (B), MG63 (C) and HeLa (D) cells transfected with reporter plasmids and pMT-2Tax. After sonication, immunoprecipitation was performed with the antibodies indicated. Precipitated DNA fragments were subjected to PCR with primers specific for the gpκB and IgκB sites in plasmids. The PCR products were 369-bp and 449-bp in length for the gpκB and IgκB sites, respectively.

bovine serum (FBS) with penicillin G (1000 U/ml) and streptomycin (10 μg/ml). Huh7 and HepG2 cells were cultured in DMEM-high glucose (D5796, Sigma-Aldrich) with 10% FBS and antibiotics (Sainz et al., 2009; Wilkening et al., 2003). C-1300 cells were cultured in RPMI1640 medium supplemented with 5% FBS and antibiotics (Fukuhara et al., 1996). Jurkat, K562 and Raji cells were cultured in RPMI1640 with 10% FBS and antibiotics (Karpova et al., 2005; Lozzio and Lozzio,1979; Schneider et al., 1977). TNFα was added to REF52 cell culture for 30 min at a concentration of 40 ng/ml otherwise stated. Cells were cultured at 37 °C in humidified atmosphere with 5% CO_2 in air.

Plasmids

The reporter plasmids used were pIgκB-Luc and pgpκB-Luc carrying three tandem repeats of κB sites in the immunoglobulin light chain (IgκB: 5' –GGGGACTTTCC–3') and gp34 (OX40L) (gpκB: 5'–GGGGAAATTCA–3') genes, respectively, in pGL3-Basic vector (Promega) with the gp34 (OX40L) core promoter (from −31 to +27) (Ohtani et al., 1998). Expression plasmids of NF-κB subunits were R/C CMV RelA for RelA/p65, R/C CMV p50 for p50, R/C CMV RelBM2 for RelB, pCM-p52 for p52, pCn100 for p100 and pEF/c-Rel for c-Rel (Baker et al., 1990; Latimer et al., 1998; Nakayama et al., 1992; Tripathi and Aggarwal, 2006; Yamaoka et al., 1996). The Tax1 expression plasmids pMT-2Tax and pEFneoTax1, and the expression plasmids for wild type Tax2B and a chimeric mutant of Tax1 and Tax2 (Tax1/2) have been described previously (Matsumoto et al., 1997; Shoji et al., 2009). The β-galactosidase expression plasmid pCMV-β-gal was used as an internal control of transfection (Gunning et al., 1987; Matsumoto et al., 1994).

Antibody

Antibodies to NF-κB subunits (RelA, SC-372; p50, SC-114; RelB, SC-19 and p52, SC-848), anti-C23 antibody (H-250), anti-IκBα antibody (SC-371) and anti-β-tubulin antibody (H-235) were purchased from Santa Cruz. Anti-Tax1 mouse monoclonal antibody TAXY-7 is described elsewhere (Tanaka et al., 1991). Anti-phospho-IκBα antibody (5A5) was obtained from Cell Signaling. Fluorescein isothiocyanate (FITC)-conjugated anti-rabbit IgG antibody (eBioscience) and Texas Red-conjugated anti-mouse IgG antibody (Vector) were used for visualization.

Luciferase reporter assay

REF52 and MG63 cells were transfected with 5 μg of plasmid DNA in 2 × HEPES buffered saline with 0.25 M $CaCl_2$ 24 h after cell plating in a 10 cm dish. Jurkat, K562 and Raji cells were transfected with 5 μg of plasmid DNA in DEAE-dextran solution [5 mg/ml in 1 M Tris–HCl (pH 7.4)]. Cells were harvested for reporter assays 48 h post transfection. C-1300, Huh7, HepG2, HeLa and 293T cells were transfected with 1 μg of plasmid DNA using Lipofectamine™ 2000 (Invitrogen) and harvested 24 h after transfection. Luciferase activity was measured with a luminometer (LB 9507, Lumat) using the Luciferase Assay System (Promega) and the activity of luciferase was normalized to β-galactosidase activity which was measured by absorption at 410 nm, or to protein content which was determined by absorption at 750 nm with a spectrophotometer (DU 64, Beckman). Assays were performed at least three times in triplicate. The means ± SE are presented.

Small-interfering RNA (siRNA)

REF52 cells was plated on a 12 well plate and incubated with siRNA (Santa Cruz) for RelB (SC-36403), p52 (SC-36043), RelA (SC-61876) and p50 (SC-156175) at a final concentration of 10 nM in Lipofectamine™ RNAiMAX (Invitrogen) at 37 °C for 6 h. Cells were cultured in medium with 10% FBS and antibiotics for 24 h, transfected with pIgκB-Luc along with pMT-2Tax in Lipofectamine 2000. Cells were further cultured for 24 h and harvested for luciferase activity measurement.

Electrophoretic mobility shift assay (EMSA)

Nuclear and cytoplasmic lysates were prepared from cells transfected with or without the indicated expression plasmids as described (Adachi et al., 1998). From each lysate, 5 μg protein were incubated with [^{32}P]-labeled probes containing κB binding (IgκB and gpκB) sites in DNA-binding buffer [13 mM HEPES (pH 7.8), 8% glycerol, 65 mM NaCl, 1 mM DTT, 0.15 mM EDTA and 1 μg of poly (dI-dC)]. In supershift assays, antibodies (1 μg) were added 1 h before probe addition. The reaction products were separated on 4% polyacrylamide gels in 5 × TBE buffer [450 mM Tris (pH 8.0), 450 mM boric acid and 10 mM EDTA (pH 8.0)] for 4 h at 200 V. Gels were dried and autoradiographed.

Chromatin immunoprecipitation (ChIP) assay

Cells were fixed in 10% formaldehyde solution for 15 min at 37 °C. Crosslinked cells were harvested, lysed in a buffer [50 mM Tris–HCl (pH 8.1), 1% SDS and 5 mM EDTA] containing 1 mM phenylmethylsulfonyl fluoride (PMSF) and sonicated 6 times of 30 s at output 4 of Duty 80 (UD-201, Tomy). The supernatant liquid was collected by centrifugation and incubated with dilution buffer [20 mM Tris–HCl (pH 8.1), 2 mM EDTA, 150 mM NaCl and 1% Triton X-100] containing PMSF with 2 μg of salmon sperm DNA, 20 μl of normal rabbit serum (Dako) and 45 μl of rProtein A Sepharose (GE Health Bio-Science) for 2 h at 4 °C. After rProtein A Sepharose was removed from samples, 2 μg of antibody (anti-RelA, anti-p50, anti-RelB or anti-p52 antibody) was added to each sample and incubated on a rotating platform for 24 h at 4 °C. Salmon sperm DNA (2 μg) and 45 μg of rProtein A Sepharose were added to each sample and incubated for 1 h at 4 °C. DNA fragments were eluted, purified and subjected to PCR with specific primers (IgκB site, forward primer, 5'–TGGAGCGGCCGCAATAAAATA–3', reverse primer, 5'-GGGCGGAGAATGGGCGGAAACT-3' gpκB site, forward primer, 5'-CGGGCCTCTTCGCTATTAG-3' reverse primer, 5'-GCGCCGGGCCTTTCTTTATGTTTT-3'). PCR products were electrophoresed on 2% agarose gels.

Western blotting assay

Cells transfected with or without pMT-2Tax were harvested for preparation of nuclear and cytoplasmic lysates. Cells were lysed with buffer A [10 mM HEPES (pH 7.8), 1.5 mM $MgCl_2$, 10 mM KCl, 0.1% NP-40, 1 mM DTT and 0.5 mM PMSF] and centrifuged to separate nuclei from supernatants. The resultant supernatants were used as sources of cytoplasmic lysates after addition of glycerol and KCl at final concentrations of 20% and 100 mM, respectively. Nuclear lysates were prepared by extraction from nuclei with buffer C [50 mM HEPES (pH 7.8), 420 mM KCl, 0.1 mM EDTA, 5 mM $MgCl_2$, 2% glycerol, 1 mM DTT and 0.5 mM PMSF]. Electrophoresis was performed with 20 μg of protein on 9% polyacrylamide gels. Proteins were blotted into membranes (AE-6667, Atto). Membranes were immunostained and visualized with antibodies using Enhanced Chemi Luminescence (ECL) (Amersham Biosciences).

Immunofluorescence staining

Cells were plated on cover glasses, fixed with 10% paraformaldehyde in PBS, and permeabilized with 0.4% Triton X-100 in PBS. Cells were incubated in 3% bovine serum albumin fraction V in PBS for 30 min and further incubated with mouse anti-Tax1 monoclonal antibody (TAXY-7) at 5 μg/ml for 1 h followed by the addition of Texas Red-conjugated anti-mouse IgG antibody. Anti-RelA, anti-p50, anti-RelB and anti-p52 antibodies were used at 5 μg/ml with FITC-conjugated anti-rabbit IgG antibody. Cells were examined with a laser scanning confocal microscope (FV10i, Olympus).

Statistical analysis

Differences in means between samples and controls were assessed for statistical significance by the student's t-test. Values less than 0.05 are taken statistically significant.

Acknowledgments

We thank J. Inoue and S. Yamaoka for providing NF-κB expression plasmids, and W. Hall for a Tax2 clone. We are grateful to L. Preston for critical reading of the manuscript.

Appendix A. Supporting information

Supplementary data associated with this article can be found in the online version at http://dx.doi.org/10.1016/j.virol.2013.04.032.

References

Adachi, O., Kawai, T., Takeda, K., Matsumoto, M., Tsutui, H., Sakagami, M., Nakanishi, K., Akira, S., 1998. Targeted disruption of the *MyD88* gene results in loss of IL-1- and IL-18-mediated function. Immunity 9, 143–150.

Akagi, T., Ono, H., Shimotohno, K., 1995. Characterization of T cells immortalized by Tax1 of human T-cell leukemia virus type 1. Blood 86, 4243–4249.

Baker, S.J., Markowitz, S., Fearon, E.R., Willson, J.K., Vogelstein, B., 1990. Suppression of human colorectal carcinoma cell growth by wild-type p53. Science 249, 912–915.

Ballard, D.W., Bohnlein, E., Lowenthal, J.W., Wano, Y., Franza, B.R., Greene, W.C., 1988. HTLV-I Tax induces cellular proteins that activate the κB element in the IL-2 receptor α gene. Science 241, 1652–1655.

Baum, P.R., Gayle, R.B., Ramsdell, F., Srinivasan, S., Sorensen, R.A., Watson, M.L., Seldin, M.F., Baker, E., Sutherland, G.R., Clifford, K.N., 1994. Molecular characterization of murine and human OX40/OX40 ligand systems: identification of a human OX40 ligand as the HTLV-1-regulated protein gp34. EMBO J. 13, 3992–4001.

Ben-Neriah, Y., Karin, M., 2011. Inflammation meets cancer, with NF-κB as the matchmaker. Nat. Immunol. 12, 715–723.

Fujii, M., Tsuchiya, H., Chuhjo, T., Akizawa, T., Seiki, M., 1992. Interaction of HTLV-1 Tax1 with p67^{SRF} causes the aberrant induction of cellular immediate early genes through CArG boxes. Genes Dev. 6, 2066–2076.

Fukuhara, S., Mukai, H., Kako, K., Nakamura, K., Munekata, E., 1996. Further identification of neurokinin receptor types and mechanisms of calcium signaling evoked by neurokinins in the murine neuroblastoma C1300 cell line. J. Neurochem. 67, 1282–1292.

Geleziunas, R., Ferrell, S., Lin, X., Mu, Y., Cunningham Jr., E.T., Grant, M., Connelly, M. A., Hambor, J.E., Marcu, K.B., Greene, W.C., 1998. Human T-cell leukemia virus type 1 Tax induction of NF-κB involves activation of the IκB kinase α (IKKα) and IKKβ cellular kinases. Mol. Cell. Biol. 18, 5157–5165.

Giam, C.Z., Jeang, K.T., 2007. HTLV-1 Tax and adult T-cell leukemia. Front. Biosci. 12, 1496–1507.

Grossman, W.J., Kimata, J.T., Wong, F.H., Zutter, M., Ley, T.J., Ratner, L., 1995. Development of leukemia in mice transgenic for the tax gene of human T-cell leukemia virus type I. Proc. Natl. Acad. Sci. USA 92, 1057–1061.

Gunning, P., Muscat, G., Ng, S.Y., Kedes, L., 1987. A human β-actin expression vector system directs high-level accumlation of antisense transcripts. Proc. Natl. Acad. Sci. USA 84, 4831–4835.

Harhaj, E.W., Harhaj, N.S., 2005. Mechanisms of persistent NF-κB activation by HTLV-I Tax. IUBMB Life 57, 83–91.

Harhaj, E.W., Sun, S.C., 1999. IKKγ serves as a docking subunit of the IκB kinase (IKK) and mediates interaction of IKK with the human T-cell leukemia virus Tax protein. J. Biol. Chem. 274, 22911–22914.
Higuchi, M., Fujii, M., 2009. Distinct functions of HTLV-1 Tax1 from HTLV-2 Tax2 contribute key roles to viral pathogenesis. Retrovirology 6, 117.
Higuchi, M., Tsubata, C., Kondo, R., Yoshida, S., Takahashi, M., Oie, M., Tanaka, Y., Mahieux, R., Matsuoka, M., Fujii, M., 2007. Cooperation of NF-κB2/p100 activation and the PDZ domain binding motif signal in human T-cell leukemia virus type 1 (HTLV-1) Tax1 but not HTLV-2 Tax2 is crucial for interleukin-2-independent growth transformation of a T-cell line. J. Virol. 81, 11900–11907.
Hinuma, Y., Nagata, K., Hanaoka, M., Nakai, M., Matsumoto, T., Kinoshita, K.I., Shirakawa, S., Miyoshi, I., 1981. Adult T-cell leukemia: antigen in an ATL cell line and detection of antibodies to the antigen in human sera. Proc. Natl. Acad. Sci. USA 78, 6476–6480.
Ishii, N., Takahashi, K., Soroosh, P., Sugamura, K., 2010. OX40-OX40 ligand interaction in T-cell-mediated immunity and immunopathology. Adv. Immunol. 105, 63–98.
Jin, D.Y., Giordano, V., Kibler, H., Nakano, H., Jeang, K.T., 1999. Role of adapter function in oncoprotein-mediated activation of NF-κB. Human T-cell leukemia virus type I Tax interacts directly with IκB kinase γ. J. Biol. Chem. 274, 17402–17405.
Karpova, M.B., Schoumans, J., Ernberg, I., Henter, J.I., Nordenskjöld, M., Fadeel, B., 2005. Raji revisited: cytogenetics of the original Burkitt's lymphoma cell line. Leuk. Res. 19, 159–161.
Latimer, M., Ernst, M.K., Dunn, L.L., Drutskaya, M., Rice, N.R., 1998. The N-terminal domain of IκBα masks the nuclear localization signal(s) of p50 and c-Rel homodimers. Mol. Cell. Biol. 18, 2640–2649.
Lenzmeier, B.A., Giebler, H.A., Nyborg, J.K., 1998. Human T-cell leukemia virus type 1 Tax requires direct access to DNA for recruitment of CREB binding protein to the viral promoter. Mol. Cell. Biol. 18, 721–731.
Lozzio, B.B., Lozzio, C.B., 1979. Properties and usefulness of the original K-562 human myelogenous leukemia cell line. Leuk. Res. 3, 363–370.
Matsumoto, K., Shibata, H., Fujisawa, J.I., Inoue, H., Hakura, A., Tsukahara, T., Fujii, M., 1997. Human T-cell leukemia virus type 1 Tax protein transforms rat fibroblasts via two distinct pathways. J. Virol. 71, 4445–4451.
Matsumoto, K., Akashi, K., Shibata, H., Yutsudo, M., Hakura, A., 1994. Single amino acid substitution (58Pro→Ser) in HTLV-1 tax results in loss of ras cooperative focus formation in rat embryo fibroblasts. Virology 200, 813–815.
Matsuoka, M., Jeang, K.T., 2007. Human T-cell leukaemia virus type 1 (HTLV-1) infectivity and cellular transformation. Nat. Rev. Cancer 7, 270–280.
Miura, S., Ohtani, K., Numata, N., Niki, M., Ohbo, K., Ina, Y., Gojobori, T., Tanaka, Y., Tozawa, H, Nakamura, M., Sugamura, K., 1991. Molecular cloning and characterization of a novel glycoprotein, gp34, that is specifically induced by the human T-cell leukemia virus type I transactivator p40 Tax. Mol. Cell. Biol. 11, 1313–1325.
Mizuguchi, M., Hara, T. and Nakamura, M., Roles of HTLV-1 Tax in leukemogenesis of human T-cells. Intech, T-Cell Leukemia, Rijeka, Croatia, 2011, pp. 51–64.
Mizuguchi, M., Asao, H., Hara, T., Higuchi, M., Fujii, M., Nakamura, M., 2009. Transcriptional activation of the interleukin-21 gene and its receptor gene by human T-cell leukemia virus type 1 Tax in human T-cells. J. Biol. Chem. 284, 25501–25511.
Nakayama, K., Shimizu, H., Watanabe, T., Okamoto, S., Yamamoto, K., 1992. A lymphoid cell-specific nuclear factor containing c-Rel-like proteins preferentially interacts with interleukin-6 κB-related motifs whose activities are repressed in lymphoid cells. Mol. Cell. Biol. 12, 1736–1746.
Niinuma, A., Higuchi, M., Takahashi, M., Oie, M., Tanaka, Y., Gejyo, F., Tanaka, F., Sugamura, K., Xie, L.P., Green, L., Fujii, M., 2005. Aberrant activation of the interleukin-2 autocrine loop through the nuclear factor of activated T cells by nonleukemogenic human T-cell leukemia virus type 2 but not by leukemogenic type 1 virus. J. Virol. 79, 11925–11934.
Ohtani, K., Nakamura, M., 2002. Molecular mechanism of Tax-mediated cell growth of human T lymphocytes. Gann Monogr. Cancer Res. 50, 50–67.
Ohtani, K., Tsujimoto, A., Tsukahara, T., Numata, N., Miura, S., Sugamura, K., Nakamura, M., 1998. Molecular mechanisms of promoter regulation of the gp34 gene that is trans-activated by an oncoprotein Tax of human T cell leukemia virus type I. J. Biol. Chem. 273, 14119–14129.
Ohtani, K., Iwanaga, R., Arai, M., Huang, Y., Matsumura, Y., Nakamura, M., 2000. Cell type-specific E2F activation and cell cycle progression induced by the oncogene product Tax of human T-cell leukemia virus type I. J. Biol. Chem. 275, 11154–11163.
Osame, M., Usuku, K., Izumo, S., Ijichi, N., Amitani, H., Igata, A., Matsumoto, M., Tara, M., 1986. HTLV-I associated myelopathy, a new clinical entity. Lancet 1, 1031–1032.
Poiesz, B.J., Ruscetti, F.W., Gazdar, A.F., Bunn, P.A., Minna, J.D. and Gallo, R.C., 1980. Detection and isolation of type C retrovirus particles from fresh and cultured lymphocytes of a patient with cutaneous T-cell lymphoma. Proc. Natl. Acad. Sci. USA 77, 7415–7419.
Qu, Z., Xiao, G., 2011. Human T-cell lymphotropic virus: a model of NF-κB-associated tumorigenesis. Viruses 3, 714–749.
Ross, T.M., Pettiford, S.M., Green, P.L., 1996. The tax gene of human T-cell leukemia virus type 2 is essential for transformation of human T lymphocytes. J. Virol. 70, 5194–5202.
Schneider, U., Schwenk, H.U., Bornkamm, G., 1977. Characterization of EBV-genome negative "null" and "T" cell lines derived from children with acute lymphoblastic leukemia and leukemic transformed non-Hodgkin lymphoma. Int. J. Cancer 19, 621–626.
Sainz, B., TenCate, V., Uprichard, S.L., 2009. Three-dimensional Huh7 cell culture system for the study of Hepatitis C virus infection. Virol. J. 6, 103.
Shoji, T., Higuchi, M., Kondo, R., Takahashi, M., Oie, M., Tanaka, Y., Aoyagi, Y., Fujii, M., 2009. Identification of a novel motif responsible for the distinctive transforming activity of human T-cell leukemia virus (HTLV) type 1 Tax1 protein from HTLV-2 Tax2. Retrovirology 6, 83.
Tanaka, Y., Inoi, T., Tozawa, H., Yamamoto, N., Hinuma, Y., 1985. A glycoprotein antigen detected with new monoclonal antibodies on the surface of human lymphocytes infected with human T-cell leukemia virus type-I (HTLV-I). Int. J. Cancer 36, 549–555.
Tanaka, Y., Yoshida, A., Tozawa, H., Shida, H., Nyunoya, H., Shimotohono, K., 1991. Production of a recombinant human T-cell leukemia virus type-I transactivator (tax1) antigen and its utilization for generation of monoclonal antibodies against various epitopes on the tax1 antigen. Int. J. Cancer 48, 623–630.
Tripathi, P., Aggarwal, A., 2006. NF-κB transcription factor: a key player in the generation of immune response. Curr. Sci. 90, 519–527.
Wilkening, S., Stahl, F., Bader, A., 2003. Comparison of primary human hepatocytes and hepatoma cell line HepG2 with regard to their biotransformation properties. Drug Metab. Dispos. 31, 1035–1042.
Xiao, G., Cvijic, M.E., Fong, A., Harhaj, E.W., Uhlik, M.T., Waterfield, M., Sun, S., 2001. Retroviral oncoprotein Tax induces processing of NF-κB2/p100 in T cells: evidence for the involvement of IKK. EMBO J. 20, 6805–6815.
Yamaoka, S., Inoue, H., Sakurai, M., Sugiyama, T., Hazama, M., Yamada, T., Hatanaka, M., 1996. Constitutive activation of NF-κB is essential for transformation of rat fibroblasts by the human T-cell leukemia virus type I Tax protein. EMBO J. 15, 873–887.
Yoshida, M., Miyoshi, I., Hinuma, Y., 1982. Isolation and characterization of retorovirus from cell lines of human adult T-cell leukemia and its implication in the disease. Proc. Natl. Acad. Sci. USA 79, 2031–2035.
Yoshida, M., 2001. Multiple viral strategies of HTLV-1 for dysregulation of cell growth control. Ann. Rev. Immunol. 19, 475–496.
Zhao, L.J., Giam, C.Z., 1992. Human T-cell lymphotropic virus type I (HTLV-I) transcriptional activator, Tax, enhances CREB binding to HTLV-I 21-base-pair repeats by protein-protein interaction. Proc. Natl. Acad. Sci. USA 89, 7070–7074.

Regular Article

LYMPHOID NEOPLASIA

HTLV-1 Tax oncoprotein stimulates ROS production and apoptosis in T cells by interacting with USP10

Masahiko Takahashi,[1] Masaya Higuchi,[1] Grace Naswa Makokha,[1] Hideaki Matsuki,[1] Manami Yoshita,[1] Yuetsu Tanaka,[2] and Masahiro Fujii[1]

[1]Division of Virology, Niigata University Graduate School of Medical and Dental Sciences, Niigata, Japan; and [2]Department of Immunology, Graduate School and Faculty of Medicine, University of the Ryukyus, Nishihara, Okinawa, Japan

Key Points

- Interaction of HTLV-1 Tax with USP10 reduces arsenic-induced stress granule formation and enhances ROS production.
- USP10 controls sensitivities of leukemia cell lines to arsenic-induced apoptosis.

Human T-cell leukemia virus type 1 (HTLV-1) is the etiological agent of adult T-cell leukemia (ATL), and the viral oncoprotein Tax plays key roles in the immortalization of human T cells, lifelong persistent infection, and leukemogenesis. We herein identify the ubiquitin-specific protease 10 (USP10) as a Tax-interactor in HTLV-1–infected T cells. USP10 is an antistress factor against various environmental stresses, including viral infections and oxidative stress. On exposure to arsenic, an oxidative stress inducer, USP10 is recruited into stress granules (SGs), and USP10-containing SGs reduce reactive oxygen species (ROS) production and inhibit ROS-dependent apoptosis. We found that interaction of Tax with USP10 inhibits arsenic-induced SG formation, stimulates ROS production, and augments ROS-dependent apoptosis in HTLV-1–infected T cells. These findings suggest that USP10 is a host factor that inhibits stress-induced ROS production and apoptosis in HTLV-1–infected T cells; however, its activities are attenuated by Tax. A clinical study showed that combination therapy containing arsenic is effective against some forms of ATL. Therefore, these findings may be relevant to chemotherapy against ATL. (*Blood.* 2013;122(5):715-725)

Introduction

Environmental stresses, such as hypoxia, heat shock, UV irradiation, and arsenite, induce several alterations in cells, such as DNA damage and accumulation of misfolded proteins, the short- and long-term consequences of which include survival of cells with aberrant DNA and protein alterations, inflammation, aging, and carcinogenesis. On the other hand, cells activate several defense mechanisms to protect against these outcomes. For instance, cells transiently induce the formation of cytoplasmic RNA granules designated as stress granules (SGs).[1,2] SGs have several antistress functions. The stresses induce translational arrest, leading to polysome disassembly, and SGs transiently store translationally inactive messenger RNAs released from polysomes and promote the translation of stress-repairing proteins, such as heat shock proteins. In addition, SGs inhibit reactive oxygen species (ROS) production and ROS-dependent apoptosis,[3] and in the meantime, cells repair altered DNA and remove misfolded proteins. Therefore, SGs play critical roles in protecting against stress-induced alterations in cells.

Viral infections have also been shown to induce the formation of SGs in host cells, although some viruses encode proteins that inhibit the formation of SGs.[4] For instance, the poliovirus-encoded protease 3C protein prevents SG formation via protease-dependent cleavage of Ras-GTPase–activating protein-binding protein 1 (G3BP1),[5] which is essential for SG assembly.[6] In addition, the NS1 encoded by the influenza A virus inhibits SG formation by preventing the activation of protein kinase that initiates a phosphorylation cascade leading to SG formation after viral infection.[7] On the basis of these observations, SGs are proposed to be involved in innate immunity against viral infections, and the inhibition of SG formation stimulates viral replication and production and augments inflammation and tissue damage.[8]

Human T-cell leukemia virus type 1 (HTLV-1) is an etiologic agent of adult T-cell leukemia (ATL).[9] Accumulation of genetic and epigenetic aberrations in HTLV-1–infected cells is a crucial step for ATL development, as only 5% of HTLV-1–infected individuals go on to have ATL at an average of 40 years after infection. Indeed, ATL cells have multiple DNA alterations, such as mutations of cellular oncogenes and tumor suppressor genes. HTLV-1 encodes the Tax oncoprotein, which plays crucial roles in the immortalization of virus-infected T cells, accumulation of gene mutations in infected cells, and leukemogenesis.[9,10] To perform such pleiotropic functions, Tax exhibits a variety of activities, including transcriptional activation of a number of cellular genes via the actions of transcription factors nuclear factor κB (NF-κB), cAMP response element binding/activating transcription factor (CREB/ATF), and AP-1 and inactivation of the tumor suppressor gene p53.[11-13] Notably, Tax also inhibits SG formation[14]; however, its significance in HTLV-1 pathogenicity remains to be clarified.

Ubiquitin-specific protease 10 (USP10) is a component of SGs that plays critical roles in several SG-mediated activities. USP10 is not essential for SG formation; however, its knockout in mouse

Submitted March 27, 2013; accepted June 3, 2013. Prepublished online as *Blood* First Edition paper, June 17, 2013; DOI 10.1182/blood-2013-03-493718.

The online version of this article contains a data supplement.

The publication costs of this article were defrayed in part by page charge payment. Therefore, and solely to indicate this fact, this article is hereby marked "advertisement" in accordance with 18 USC section 1734.

embryonic fibroblasts (MEFs) reduces SG formation, augments ROS production, and enhances ROS-dependent apoptosis.[3] In our current study, we identified USP10 as a novel binding partner of Tax protein. The activities of Tax mutants and knockdown of USP10 indicated that Tax, by interacting with USP10, inhibits SG formation and stimulates ROS production. Accumulating evidence indicates that aberrant ROS production is a factor promoting gene mutations that cause malignancy.[15] Therefore, the present findings indicate that USP10 is a host factor that inhibits ROS-induced aberration of HTLV-1–infected T cells, including genetic mutations. Notably, a previous clinical study showed that combination therapy containing arsenic trioxide, an anhydrous form of arsenite, exhibits promising effects against some forms of ATL.[16] Our results revealed that knockdown of USP10 augments arsenite-induced ROS-dependent apoptosis in HTLV-1–infected T cells. Therefore, USP10 controls the sensitivity of ATL cells to arsenic and is hence a novel target for chemotherapy against ATL.

Methods

Reagents and antibodies

The following reagents were purchased from the indicated companies: sodium arsenite (Wako Pure Chemical Industries), arsenic trioxide (Sigma-Aldrich), puromycin (Calbiochem) and *N*-acetylcysteine (NAC; Sigma-Aldrich). Arsenic trioxide was first dissolved in 1.0 N of NaOH and was then diluted with phosphate-buffered saline (PBS). The following antibodies were used in this study at the indicated dilutions: anti-USP10 (1:2000; Bethyl Laboratories), anti-HA (1:2000; Cell Signaling Technology), anti-G3BP1 (1:2000; BD Transduction Laboratories), anti-poly(A)-binding protein 1 (PABP1) (1:1000; Santa Cruz, 1:500; Abcam), anti-Tax (Taxy-7)[17] (1:1000), and anti-α-tubulin (1:1000; Oncogene).

Coimmunoprecipitation and western blot analysis

The coimmunoprecipitation and western blot analysis were performed as described previously.[3]

Immunofluorescence analysis

An immunofluorescence analysis was performed as described previously.[3] The images were analyzed with a fluorescence microscope (BZ-8000; KEYENCE). More than 300 cells in 3 random fields were analyzed using staining with SG markers, G3BP1 and USP10. The SG (%) was calculated as the ratio of SG-positive cells relative to the total number of cells.

Detection of ROS

Cellular ROS level was measured as described previously.[3] The 5-chloromethyl-2′,7′-dichlorodihydrofluorescein diacetate (CM-H_2DCFDA) fluorescence in each cell was quantified using a fluorescent analysis software package (BZ-II analyzer; KEYENCE). More than 400 cells in 4 random fields were analyzed, and the data were presented as the mean fluorescence intensity (DCFDA-F).

Quantitative determination of apoptosis

The level of apoptosis was measured according to 2 methods. First, the cells were stained with propidium iodide, and the sub-G1 DNA content was measured using flow cytometry. Second, cells cultured on coverslips in 6-well plates were fixed with 4% formaldehyde in PBS and were permeabilized with 0.1% Triton X-100 in PBS. The fixed cells were stained with Hoechst33258. After Hoechst33258 staining, the number of cells that exhibited condensed nuclei was counted using a fluorescence microscope. More than 300 cells in 3 random fields were analyzed per sample.

Statistical analysis

The data were analyzed using the unpaired Student *t* test and are presented as the mean ± standard deviation (SD). Information including "Cell lines and culture conditions," "Plasmid constructs," and the "Establishment of stable USP10-knockdown cell lines using lentiviral transduction" is provided in the supplemental Methods, available on the *Blood* Web site.

Results

Tax interacts with USP10

Cytotoxic T lymphoblast cell (CTLL)-2 is a mouse interleukin (IL)-2–dependent T-cell line. Tax transforms CTLL-2 cells from IL-2–dependent growth into IL-2–independent growth, and its activity is much higher than that of nonleukemogenic HTLV-2 Tax2.[18,19] Studies of chimeric Tax proteins including Tax2 have revealed that the C-terminal PDZ domain-binding motif (PBM) in Tax, which is missing in Tax2, is a factor responsible for the high transforming activity of CTLL-2.[18,19] To obtain information on how Tax PBM augments the Tax-induced transformation of CTLL-2, we isolated several Tax-binding proteins in CTLL-2 cell lysates using glutathione *S*-transferase fusion proteins of Tax vs TaxΔC with deletion of PBM (M.H. and M.F., unpublished observations). One such Tax-binding protein is USP10. To establish the interaction between Tax and USP10 in mammalian cells, plasmids encoding Tax as well as USP10 with a hemagglutinin (HA) epitope (HA-USP10) were transiently expressed in 293T cells, and the cell lysates were immunoprecipitated with anti-HA antibodies. The anti-HA antibody coprecipitated HA-USP10 with Tax (Figure 1A). Conversely, anti-Tax coprecipitated HA-USP10 with Tax (Figure 1B). Unexpectedly, USP10 also interacted with the Tax PBM mutant TaxΔC (Figure 1B), indicating that PBM is not essential for the interaction between Tax and USP10. In addition, Tax formed a complex with USP10 in HTLV-1–infected T cells (Figure 1C). A total of 7 HTLV-1–positive and 3 HTLV-1–negative T-cell lines constitutively expressed USP10 as well as 2 USP10-binding proteins, G3BP1[20] and PABP1,[21] and the levels of these factors did not correlate with that of Tax (Figure 1D). An immunofluorescence analysis visualized endogenous and exogenous USP10 in the cytoplasm, where some proteins colocalized with Tax (Figures 1E and 6A; as represented by arrows). Taken together, these results indicate that Tax interacts with USP10 in HTLV-1–infected T cells, and these molecules partly colocalize in the cytoplasm.

To delineate the domain of Tax that is responsible for the interaction with USP10, we examined the interactions between Tax mutants and USP10. Three of the mutants, TaxSH-1, TaxSH-2, and $Tax^{62\text{-}353}$, exhibited minimal interaction with USP10 (Figure 2A-B). TaxSH-1 and TaxSH-2 have point mutations at Pro-58 to Ser and Leu-205 to Arg, respectively. $Tax^{62\text{-}353}$ has an *N*-terminal deletion from amino acids 1 to 61, containing the zinc finger region. Therefore, both the *N*-terminal region and the central region of Tax are required for interaction with USP10. On the other hand, TaxM22 and Tax703 demonstrated equivalent USP10-binding activity to wild-type (WT) Tax and have point mutations at Gly-137 and Leu-138 and at Leu-319 and Leu-320, respectively (Figure 2A-B).

To identify the domain of USP10 responsible for the interaction with Tax, plasmids encoding various USP10 mutants were constructed (Figure 2C). An immunoprecipitation analysis of 293T cells showed that the deletion of amino acids 727 to 798 of the C-terminal region of USP10 prominently reduced binding with Tax, whereas the

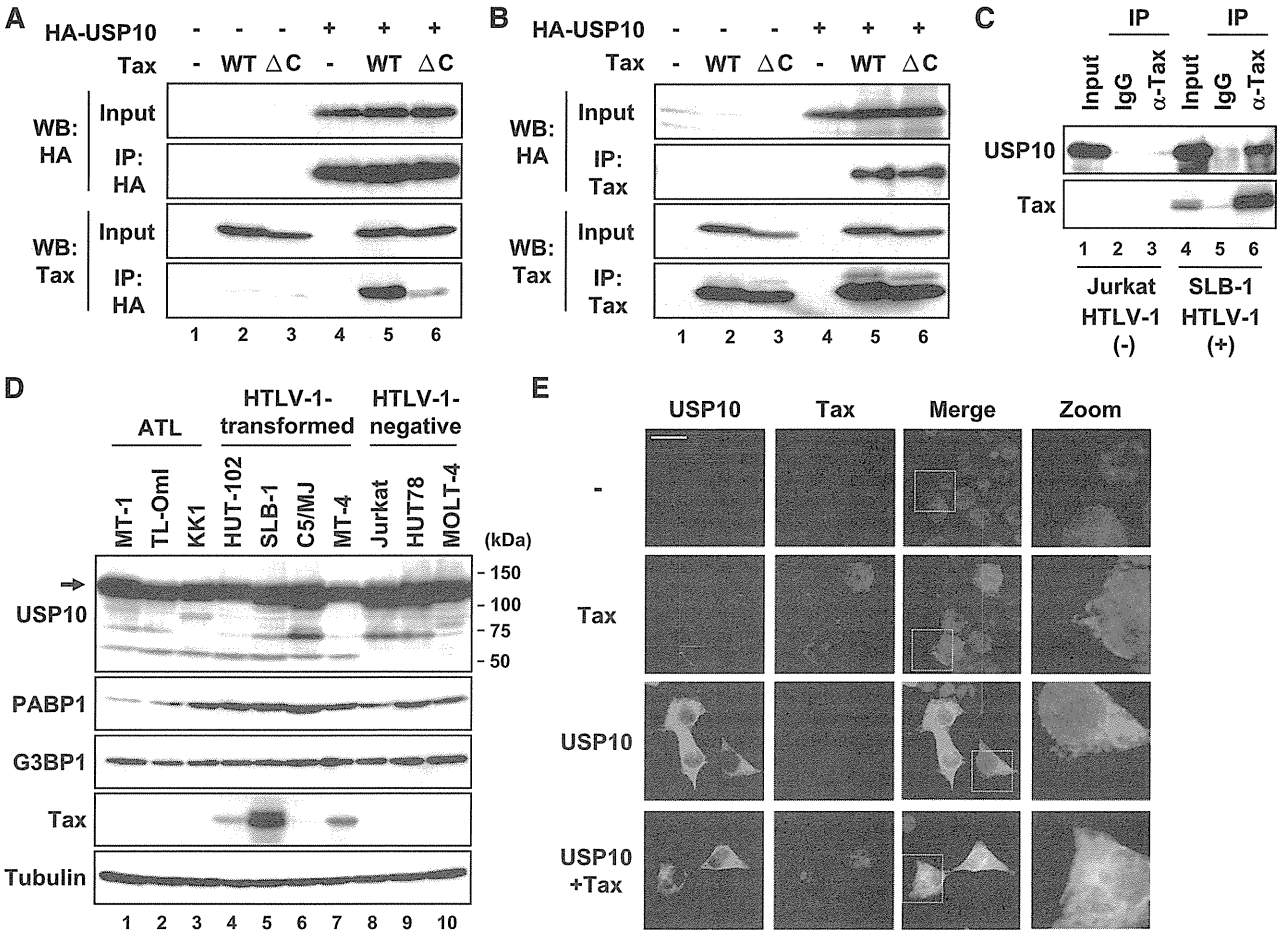

Figure 1. Tax interacts with USP10. (A,B) 293T cells were transfected with a control plasmid (lanes 1, 4), Tax plasmid (lanes 2, 5), or TaxΔC plasmid (lanes 3, 6) together with (lanes 4-6) or without (lanes 1-3) an HA-USP10 plasmid. At 48 hours after transfection, the cell lysates were immunoprecipitated with anti-HA (A) or anti-Tax (B) antibodies, and the total lysates (input) and immunoprecipitates (IP) were characterized using a western blot analysis with anti-HA and anti-Tax antibodies. TaxΔC has a 4 amino acid deletion on the Tax C-terminus, the peptide of which is missing in the nonleukemogenic HTLV-2 Tax2, because the original goal was to isolate binding factors specific to Tax but not to Tax2. (C) The cell lysates prepared from HTLV-1–uninfected T cells (Jurkat; lanes 1-3) and HTLV-1–infected T cells (SLB-1; lanes 4-6) were immunoprecipitated with anti-Tax antibodies (lanes 3, 6) or control antibodies (lanes 2, 5). The input lysate and IP were characterized using a western blot analysis with anti-USP10 and anti-Tax antibodies. (D) Cell lysates were prepared from 7 HTLV-1–infected T-cell lines (lanes 1-7) and 3 HTLV-1–uninfected T-cell lines (lanes 8-10). The expressions of USP10, PABP1, G3BP1, Tax, and α-tubulin proteins were determined using a western blot analysis with the corresponding antibodies. (E) 293T cells were transfected with a Tax plasmid together with or without the HA-USP10 plasmid. The transfected cells were stained with anti-USP10 (green) and anti-Tax (red) antibodies. The nuclei were counterstained with Hoechst33258 (blue). The bar indicates 20 μm.

deletion of amino acids 1 to 116 of the *N*-terminal region, which are essential for the formation of SGs as well as binding with G3BP1 and PABP1,[3] had a minimal effect on binding with Tax (Figure 2D), indicating that Tax interacts with amino acids 727 to 798 of USP10.

Binding of Tax with USP10 inhibits arsenite-induced SG formation

USP10 is a component of SGs that is involved in innate immunity against viral infections.[8] Intriguingly, Tax inhibits SG formation.[14] Therefore, we next investigated whether USP10 is involved in the Tax-mediated inhibition of SG formation. Arsenite, a prooxidant well known to stimulate SG formation, induced SGs in 293T cells, and USP10 was predominantly detected in the formed SGs (Figure 3A). The 293T cells were then transiently transfected with expression vectors encoding WT Tax, $Tax^{62\text{-}353}$, TaxSH-1, or TaxSH-2, treated with arsenite and stained with anti-USP10 antibodies. WT Tax inhibited arsenite-induced SG formation (as represented by the arrow in Figure 3B). This is consistent with the findings of a previous study.[14] In addition, 2 Tax mutants (TaxM22 and Tax703) that are capable of interacting with USP10 also reduced arsenite-induced SG formation (Figure 3D). Of the 3 Tax mutants defective in USP10 binding, $Tax^{62\text{-}353}$ was completely unable to interfere with SG formation. In contrast, the other 2 Tax mutants (TaxSH-1 and TaxSH-2) inhibited SG formation; however, the inhibitory activity was half that of WT Tax (Figure 3B-C). These results suggest that Tax inhibits SG formation and that this inhibition is partly mediated through the interaction between Tax and USP10.

Tax augments arsenite-induced apoptosis of 293T cells

Because SGs inhibit arsenite-induced apoptosis,[3,22,23] we next examined whether Tax affects the sensitivity of 293T cells to arsenite-induced apoptosis. 293T cells were transfected with expression vectors encoding Tax and its mutants, and the cells were treated with 0.5 mM of arsenite for 80 minutes, washed with PBS, and further cultured for 1 hour. The cells were then stained with anti-Tax antibodies and Hoechst33258 (supplemental Figure 1). The apoptotic cells were monitored by detecting condensed nuclei in the

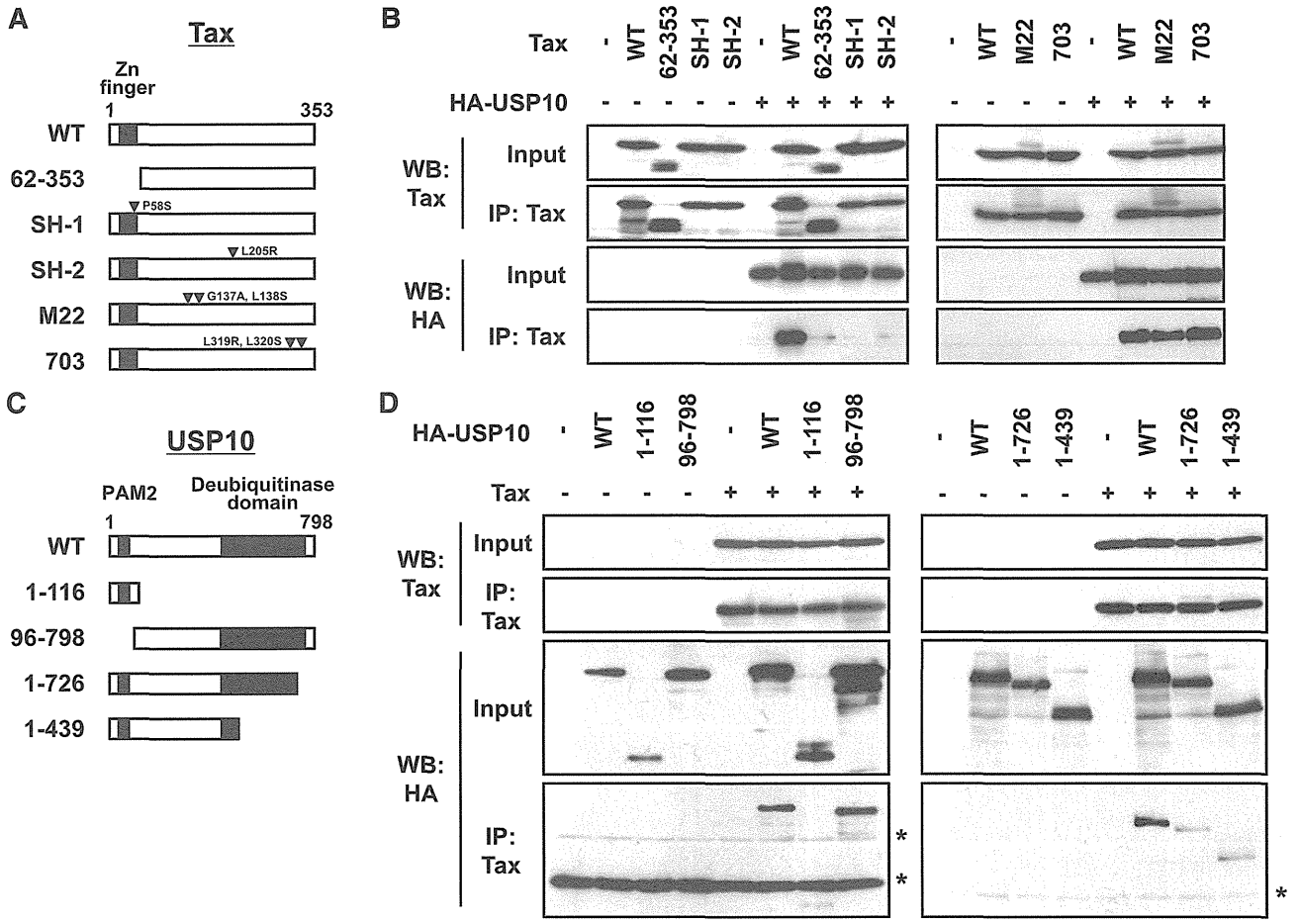

Figure 2. The domains of Tax and USP10 are required for the interaction. (A) A schematic representation of Tax and its mutants used in this study. (B) Cell lysates were prepared from 293T cells transfected with the HA-USP10 plasmid together with Tax mutant plasmids, and then were immunoprecipitated with anti-Tax. The total lysates (input) and immunoprecipitates (IP) were characterized using a western blot analysis with anti-Tax and anti-HA antibodies. (C) A schematic representation of USP10 and its mutants used in this study. PAM2 (PABP-interacting motif 2) mediates the interaction with PABP.[21] (D) 293T cells were transfected with plasmids encoding HA-tagged USP10 (HA-WT) or its mutants (HA-1-116, HA-96-798, HA-1-726, or HA-1-439), as described in (C), together with Tax plasmids. Cell lysates prepared from 293T cells were then immunoprecipitated with anti-Tax antibodies. The input and immunoprecipitates were characterized using a western blot analysis with anti-Tax and anti-HA antibodies. The asterisks indicate nonspecific bands.

Tax-expressing cells (Figure 3E). Tax augmented the arsenite-induced apoptosis of 293T cells, and this apoptosis was inhibited by an antioxidant (NAC) (Figure 3F). On the other hand, the augmentation of apoptosis induced by TaxSH-1 and TaxSH-2 in the 293T cells was approximately half that induced by WT Tax, and $Tax^{62\text{-}353}$ had a minimal effect on apoptosis (Figure 3E). These results suggest that Tax, at least in part through its interaction with USP10, augments arsenite-induced apoptosis of 293T cells, and that this apoptosis augmentation correlates with the SG inhibitory activity.

Tax stimulates ROS production via USP10 in T cells

We recently showed that USP10 downregulates steady-state ROS production in several epithelial cell lines and inhibits arsenite-induced ROS production.[3] To elucidate the role of USP10 in ROS production in T cells, we knocked down the USP10 expression in a human T-cell line (Jurkat) using short hairpin RNA (shRNA) (Figure 4A) and measured the ROS levels using staining with CM-H_2DCFDA, a redox-sensitive probe (Figure 4B). Two USP10-knockdown cells targeting different regions of *USP10* messenger RNA produced more ROS than the control cells (Figure 4C). These results suggest that endogenous USP10 in T cells downregulates ROS production under steady-state conditions.

Tax stimulates ROS production in T cells.[24] To examine whether USP10 is involved in Tax-induced ROS production in T cells, USP10-knockdown (sh-USP10-1) Jurkat and control cells (sh-NT) were infected with Tax-encoding lentivirus, and the cells were assessed for ROS production. Tax elevated ROS production in the control cells; however, this activity was abrogated by the knockdown of USP10 (Figure 4D). Two Tax mutants, TaxSH-1 and TaxSH-2, defective for USP10 interactions were unable to elevate ROS production (Figure 4D). In addition, 2 other Tax mutants (TaxM22 and Tax703) that are active for USP10 binding failed to elevate ROS production (Figure 4E). Whereas WT Tax activates the transcription of cellular genes through 2 transcription factors, NF-κB and CREB, TaxM22 is inactive for NF-κB–dependent transcriptional activation, and Tax703 exhibits a weak degree of CREB-dependent activation.[25,26] Therefore, these results suggest that transcriptional activation of cellular genes by Tax is required for the production of ROS induced by Tax. In addition, TaxΔC without PBM did not stimulate ROS production (Figure 4F). Therefore, PBM and its binding proteins are also required for Tax to stimulate ROS production. It should be noted that TaxSH-1 defective for the USP10 interaction possesses PBM and activates CREB- and NF-κB–dependent transcription equivalent to WT Tax. Taken together, these results indicate that Tax stimulates ROS production through combined

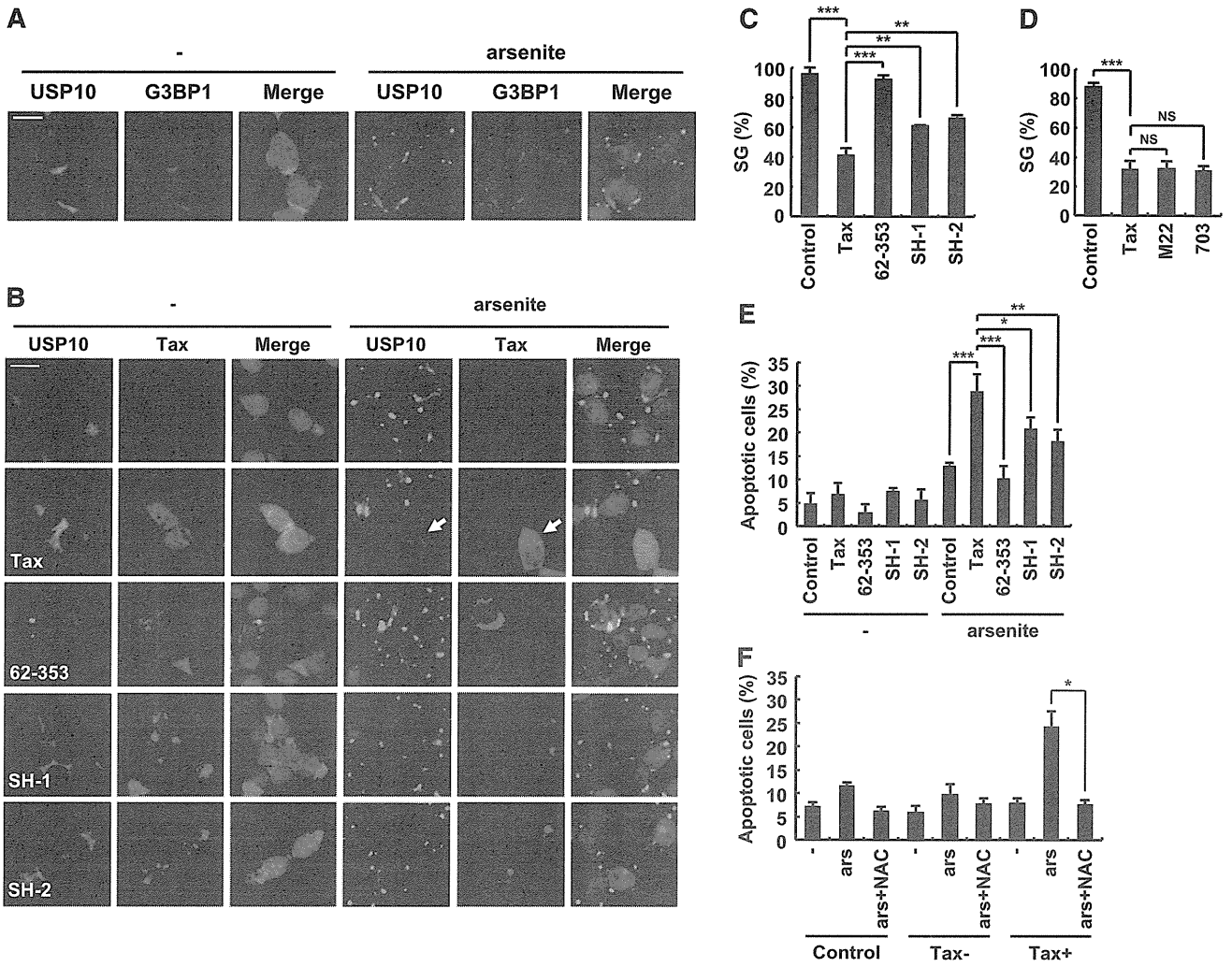

Figure 3. Tax inhibits SG formation and augments arsenite-induced apoptosis. (A) 293T cells were treated with 0.5 mM of sodium arsenite for 60 minutes and then were stained with anti-USP10 antibodies (green), anti-G3BP1 antibodies (red), and Hoechst33258 (blue). The bar indicates 20 μm. (B) 293T cells were transfected with the indicated plasmids (Tax, $Tax^{62\text{-}353}$, TaxSH-1, or TaxSH-2). The transfected cells were treated with 0.5 mM of sodium arsenite for 60 minutes and then were stained with anti-USP10 antibodies (green), anti-Tax (red) antibodies, and Hoechst33258 (blue). The arrow indicates a cell that exhibits reduced SG formation. The bar indicates 20 μm. (C,D) The SG (%) in Tax-positive cells and control cells is presented. (E) The number of cells containing condensed nuclei among the Tax-positive cells was counted. (F) 293T cells were transfected with Tax plasmids and then were incubated with or without 5 mM of NAC, treated with 0.5 mM of sodium arsenite, and stained with anti-Tax antibodies and Hoechst33258. The numbers of cells containing condensed nuclei among the Tax-positive cells and the control cells were counted. In all experiments, the values denote mean ± SD; $^*P < .05$; $^{**}P < .01$; $^{***}P < .001$; NS indicates not statistically significant.

actions by interacting with USP10 and modulating the activities of the NF-κB, CREB, and PBM pathways.

USP10 knockdown in T cells reduces SG-forming activities and augments sensitivity to arsenite-induced apoptosis

We next investigated the roles of USP10 in arsenite-induced SG formation and apoptosis in T cells. High-dose arsenite (0.25 mM) induced SG formation in 2 distinct USP10-knockdown Jurkat cells; however, the level of SGs was less than that observed in the control cells (Figure 5A-B). In addition, knockdown of USP10 augmented the apoptosis of Jurkat cells treated with or without a low dose of arsenite (5 μM) (Figure 5C). It should be noted that human T-cell lines are more sensitive to arsenite-induced apoptosis than adherent cell lines, including 293T cells, and even a concentration of arsenite (5 μM) that does not induce the formation of visible SGs can still induce apoptosis in T-cell lines, but not adherent cell lines. These results indicate that USP10 in T cells augments SG formation and reduces arsenite-induced apoptosis.

Augmented arsenite-induced apoptosis of HTLV-1–infected T cells is associated with a reduced level of SG-forming activity

A recent study showed that combination therapy containing arsenic trioxide, interferon-α, and zidovudine exhibits promising therapeutic effects on some forms of ATL.[16] In addition, arsenite induces apoptosis in HTLV-1–infected T-cell lines more so than in HTLV-1–uninfected T-cell lines.[27] Therefore, we next examined whether the high sensitivity of HTLV-1–infected T-cell lines to arsenite is related to the level of SG-forming activity. HTLV-1–infected T-cell lines treated with a low dose of arsenite exhibited more apoptosis than the HTLV-1–uninfected cell lines (Figure 6C). This apoptosis was inhibited by NAC (Figure 6D). In addition, high-dose arsenite induced SG formation in HTLV-1–infected T-cell lines, and the amount of SGs was lower than that observed in the HTLV-1–uninfected cell lines (Figure 6A-B). Moreover, USP10 knockdown in the HTLV-1–infected T-cell line MT-4 induced less arsenite-induced SG formation, more ROS production, and more arsenite-induced apoptosis than the control USP10-competent MT-4

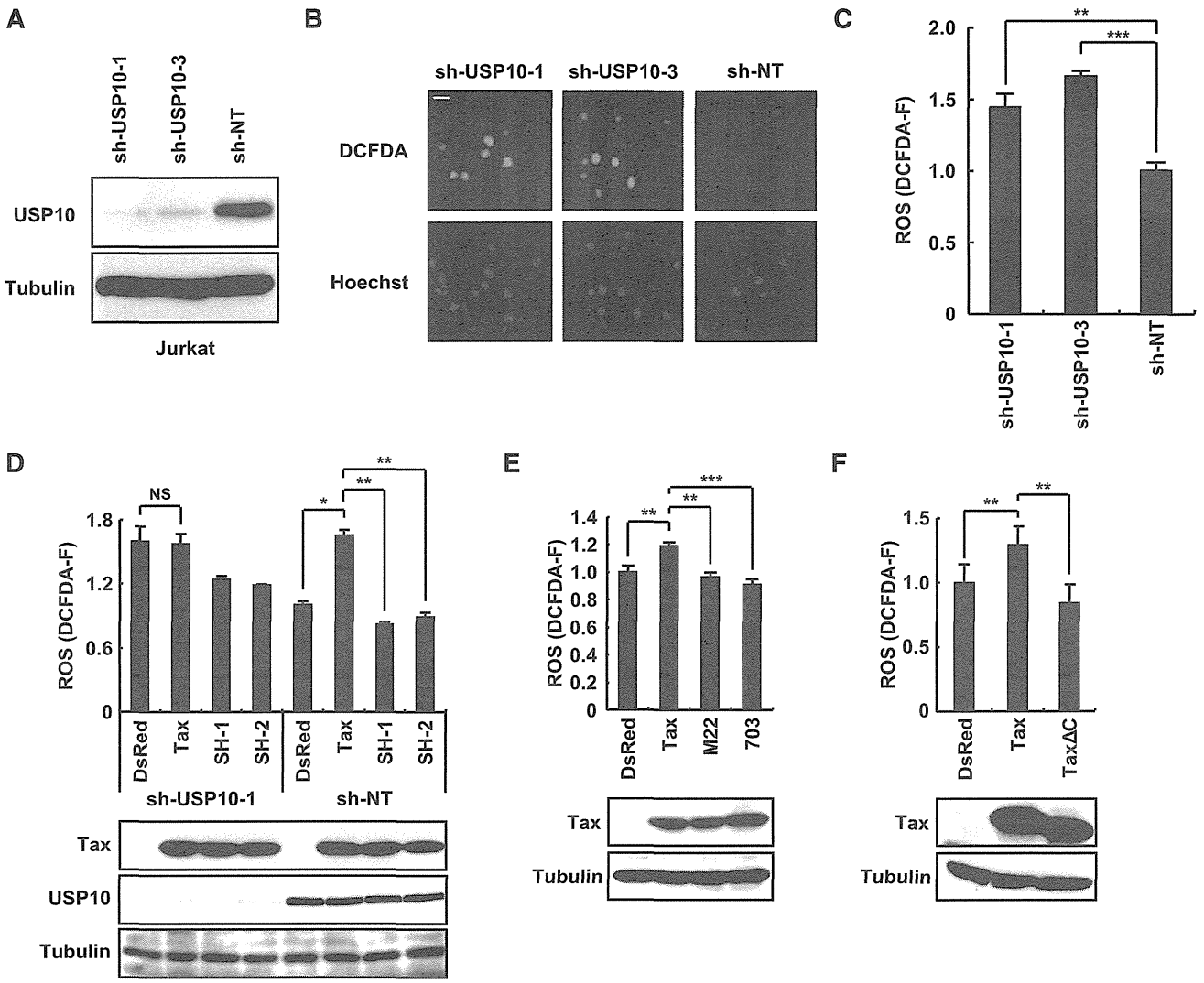

Figure 4. Tax stimulates ROS production in part through an interaction with USP10. (A) Jurkat cells were infected with lentiviruses encoding human *USP10* shRNA (sh-USP10-1 or sh-USP10-3) or control nontargeting shRNA (sh-NT), and the cells were then cultured in the presence of puromycin. Cell lysates prepared from the selected cells were characterized using a western blot analysis with anti-USP10 and anti-α-tubulin antibodies. (B) USP10-knockdown Jurkat cells and control cells were stained with 5 μM of CM-H_2DCFDA (green) and Hoechst33258 (blue) for 5 minutes at 37°C. Staining of the cells was visualized using a fluorescence microscope. The bar indicates 10 μm. (C) The ROS levels (DCFDA-F) in cells treated as in (B) were quantitatively measured using a cell imaging software program. (D-F) USP10-knockdown (sh-USP10-1) Jurkat cells and control (sh-NT) (D) or Jurkat cells (E,F) were infected with the indicated Tax lentiviruses. The infected cells were assessed for ROS production (DCFDA-F) using 5 μM of CM-H_2DCFDA. Aliquots of the above-treated cells were subjected to a western blot analysis using anti-Tax, anti-USP10, and anti-α-tubulin antibodies. In all experiments, the values denote the mean ± SD; $^*P < .05$; $^{**}P < .01$; $^{***}P < .001$; NS indicates not statistically significant.

cells (supplemental Figure 2). Collectively, these results indicate that USP10 inhibits ROS production and apoptosis in HTLV-1–infected T cells and that the inhibition correlates with the SG-forming activity.

Arsenic trioxide, an anhydrous form of arsenite, has been used as a drug against ATL in place of sodium arsenite.[28] To confirm that arsenic trioxide also exhibits similar activities to arsenite, we treated HTLV-1–uninfected (Jurkat) and infected (SLB-1) T-cell lines with arsenic trioxide. Arsenic trioxide (0.1-1.0 mM) induced SG formation in both the Jurkat and SLB-1 cells; however, the level of SG-forming activity was lower in the SLB-1 cells than in the Jurkat cells (supplemental Figure 3A). Moreover, the arsenic trioxide-induced apoptosis of the SLB-1 cells was significantly greater than that of the Jurkat cells, and the apoptosis was abrogated by treatment with NAC (supplemental Figure 3B-C). These results suggest that arsenic trioxide induces the ROS-dependent apoptosis of HTLV-1–infected T cells via the same mechanism as sodium arsenite (Figure 6).

Approximately half of leukemic cells in patients with ATL do not express a functional *tax* gene.[29] Therefore, we next examined whether 3 ATL cell lines established from patients with ATL are sensitive to arsenite-induced apoptosis. Three ATL cell lines with or without a minimal amount of a Tax protein expression demonstrated different sensitivities to arsenite-induced apoptosis, and the level of sensitivity correlated inversely with the level of SG-forming activity (Figure 7A-B). These results suggest that sensitivity to arsenite-induced apoptosis in ATL cells is also regulated by SG-forming activities. To extend this hypothesis into cell types other than T cells, we characterized the sensitivity to arsenite-induced apoptosis and the SG-forming activity of leukemia/lymphoma cell lines unrelated to ATL. The 3 B-cell lines (Ramos, Daudi, and BJAB) were derived from Burkitt lymphoma (Figure 7C-D); the next one (NB4), from promyeloid leukemia; and the last one (THP-1), from acute monocytic leukemia (Figure 7E-F). They exhibited distinct sensitivities to arsenite-induced apoptosis, and the level of sensitivity correlated

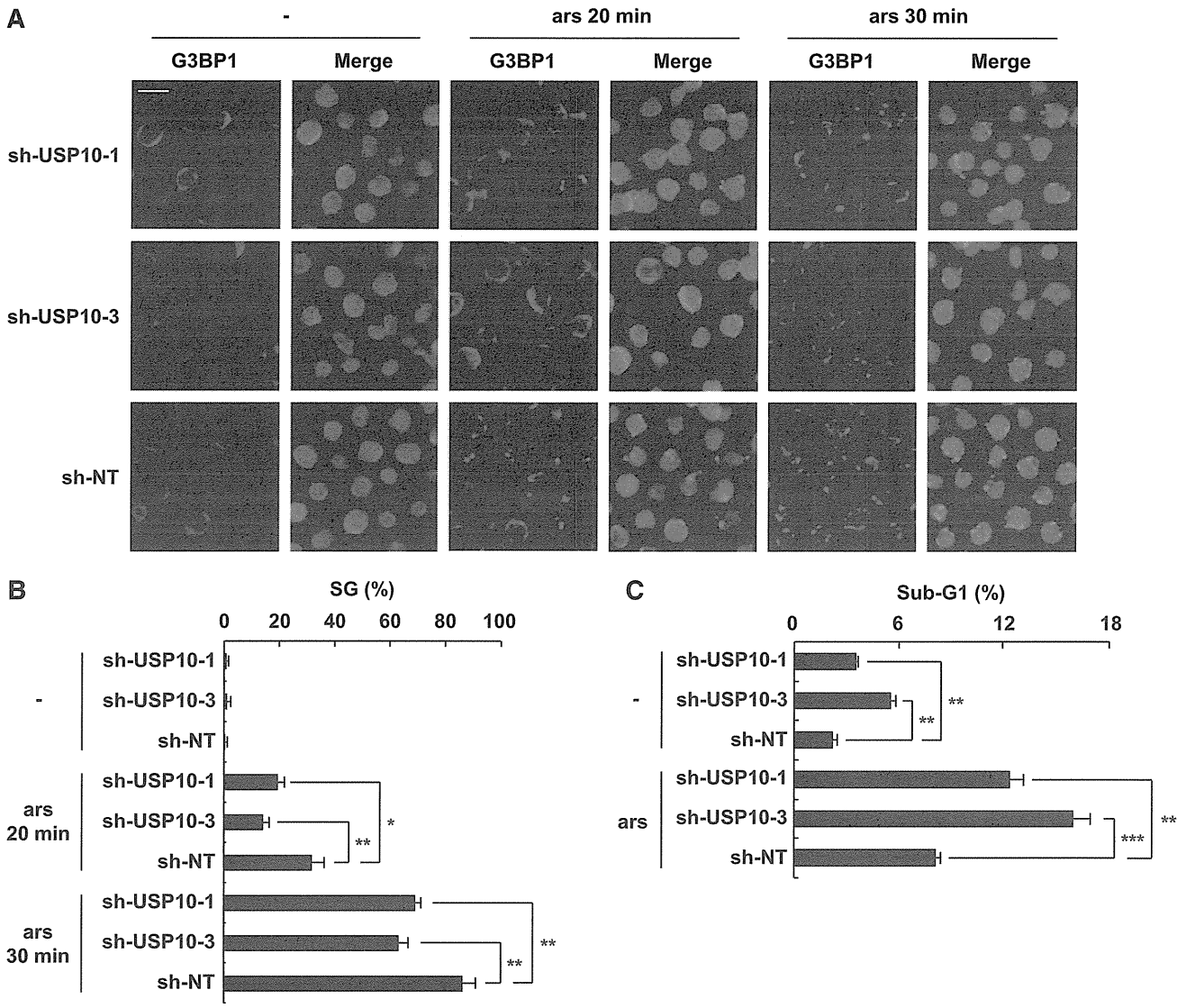

Figure 5. USP10 in T cells controls the SG-forming activity and sensitivity to arsenite-induced apoptosis. (A) USP10-knockdown Jurkat cells and control cells were treated with 0.25 mM of sodium arsenite for 0, 20, and 30 minutes and then were stained with anti-G3BP1 antibodies (red) and Hoechst33258 (blue). The bars indicate 10 μm. (B) The SG (%) is presented. (C) USP10-knockdown Jurkat cells and control cells were treated with 5 μM of sodium arsenite for 48 hours and then were stained with propidium iodide (PI). The proportion of the sub-G1 fraction was measured using flow cytometry. In all experiments, the values denote the mean ± SD; $^{*}P < .05$; $^{**}P < .01$; $^{***}P < .001$.

inversely with the level of SG-forming activity. These results further support the idea that arsenite-induced SG formation of various hematopoietic leukemic cells correlates inversely with sensitivity to arsenite-induced apoptosis.

Discussion

In our study, we identified USP10 as a novel binding protein of HTLV-1 Tax in T cells and found that Tax inhibits at least 3 USP10-associated functions, namely, SG formation, ROS suppression, and inhibition of apoptosis. Under various stress conditions, including viral infection, USP10 can prevent the emergence of cells with stress-induced ROS-dependent DNA and protein alterations.[3] Therefore, our present findings suggest that Tax, by interacting with USP10, augments ROS-dependent alterations, such as DNA damage, in HTLV-1–infected T cells, thereby promoting leukemogenesis.

Two Tax mutants (TaxSH-1 and TaxSH-2) defective for USP10 binding inhibited SG formation; however, the inhibition achieved by these mutants was half that of WT Tax. Legros et al demonstrated that Tax inhibits SG formation by binding to histone deacetylase 6 (HDAC6), a component of SGs.[14] Therefore, both USP10 and HDAC6 are likely to play a role in the Tax-induced inhibition of SG formation. On the other hand, HDAC6 is not likely to mediate Tax-induced ROS production because, unlike WT Tax, TaxSH-1 and TaxSH-2 have a minimal effect on ROS production.

The activities of the Tax mutants suggest that multiple functions of Tax, in addition to the inhibition of USP10 functions, are involved in the stimulation of ROS production. Two Tax mutants (TaxM22 and Tax703), which are defective for NF-κB- and CREB-dependent transcriptional activation, respectively, both failed to elevate ROS production (Figure 4), suggesting that Tax stimulates ROS generation via gene(s) regulated by NF-κB and CREB. Indeed, NF-κB can

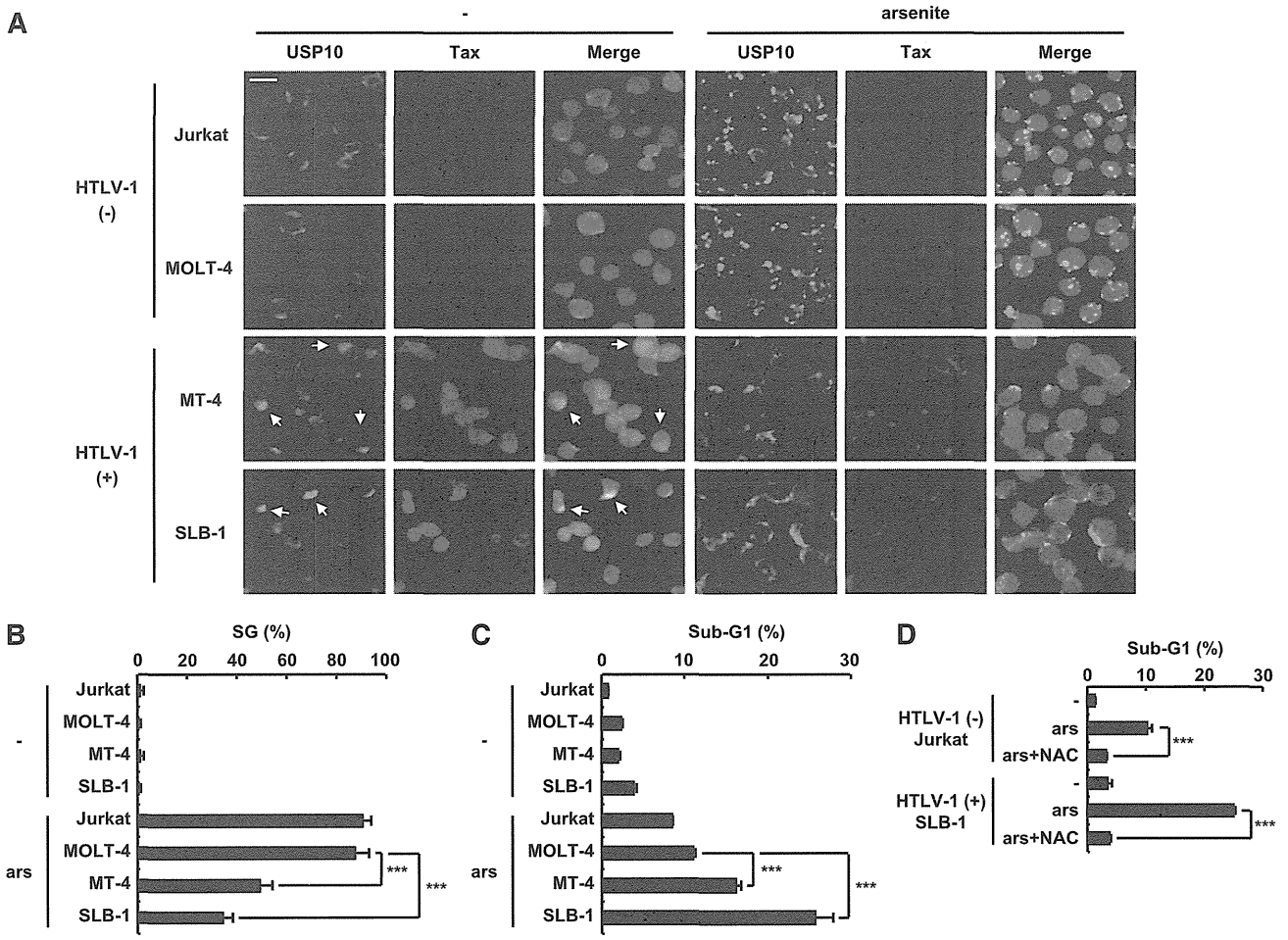

Figure 6. The level of arsenite sensitivity of HTLV-1–infected T cells correlates with the level of SG-forming activity. (A,B) HTLV-1–uninfected (Jurkat and MOLT-4) and HTLV-1–infected (SLB-1 and MT-4) T cells were treated with 0.5 mM of sodium arsenite for 30 minutes and then were stained with anti-USP10 antibodies (green), anti-Tax antibodies (red), and Hoechst33258 (blue). The arrows indicate cells with colocalization of USP10 and Tax. The bar indicates 10 μm in (A). The SG (%) in the indicated cells is presented in (B). (C) HTLV-1–uninfected (Jurkat and MOLT-4) and HTLV-1–infected (MT-4 and SLB-1) T cells were treated with 5 μM of sodium arsenite for 48 hours and then were stained with PI. The proportion of the sub-G1 population (apoptotic cells) was measured using flow cytometry. (D) Jurkat and SLB-1 cells were incubated with or without 10 mM of NAC, further treated with 5 μM of sodium arsenite for 48 hours, and stained with PI. The proportion of sub-G1 populations (%) was measured using flow cytometry. In all experiments, the values denote mean ± SD; ***$P < .001$.

activate prooxidant genes, such as the reduced NAD phosphate oxidase NOX2.[30,31] In addition, PBM was required for Tax to stimulate ROS production (Figure 4). Tax, acting through PBM, interacts with several PDZ domains containing proteins, including Dlg1, Scribble, and MAGI-1, then inactivates the functions of these PDZ proteins by altering subcellular localization.[32-35] The PDZ proteins localize near the plasma membrane and form a complex with several membrane receptors, then positively or negatively control signals from corresponding membrane receptors.[36,37] Collectively, we tentatively propose the following hypothesis of how Tax stimulates ROS production in T cells. Although Tax, acting through the NF-κB, CREB, and PBM pathways, induces the expression of prooxidant gene(s), by acting through USP10, it blocks the antioxidant response, thereby prolonging the production of ROS. A further analysis is, however, required to understand the precise mechanisms underlying how Tax stimulates ROS production in T cells.

Tax is an ubiquitinated protein, and the ubiquitination controls the stability and transcriptional activity of Tax.[38,39] Although USP10 is a Tax-interacting deubiquitinase, the overexpression of USP10 in 293T cells minimally affects the ubiquitination of Tax (H.M, M.T., and M.F., unpublished observations). In this aspect, several proteins have been shown to modulate the ubiquitination of Tax. For instance, USP20 directly deubiquitinates Tax and suppresses the NF-κB activation induced by Tax.[40] In addition, the metalloprotease STAM-binding protein-like 1 indirectly induces the deubiquitination of Tax, thereby stabilizing Tax and promoting its nuclear export.[41] On the other hand, Tax is ubiquitinated by The Really Interesting New Gene Finger Protein 4, and this ubiquitination is required for cytoplasmic localization and the activation of NF-κB.[42] Therefore, further analyses of these cellular proteins, including USP10, will clarify the precise mechanisms underlying the functions of Tax in the pathogenesis of HTLV-1.

A previous study showed that USP10 inhibits arsenite-induced ROS-dependent apoptosis in MEFs and that this inhibitory activity is mediated by the formation of USP10-containing SGs.[3] In our study, unlike MEFs, USP10 inhibited arsenite-induced ROS-dependent apoptosis in a human T-cell line, even at a concentration of arsenite that does not provoke visible SG formation. These results suggest 2 possible mechanisms. USP10 may block ROS-dependent apoptosis without forming SGs in T cells. Alternatively, a low concentration of arsenite may induce small SGs undetectable

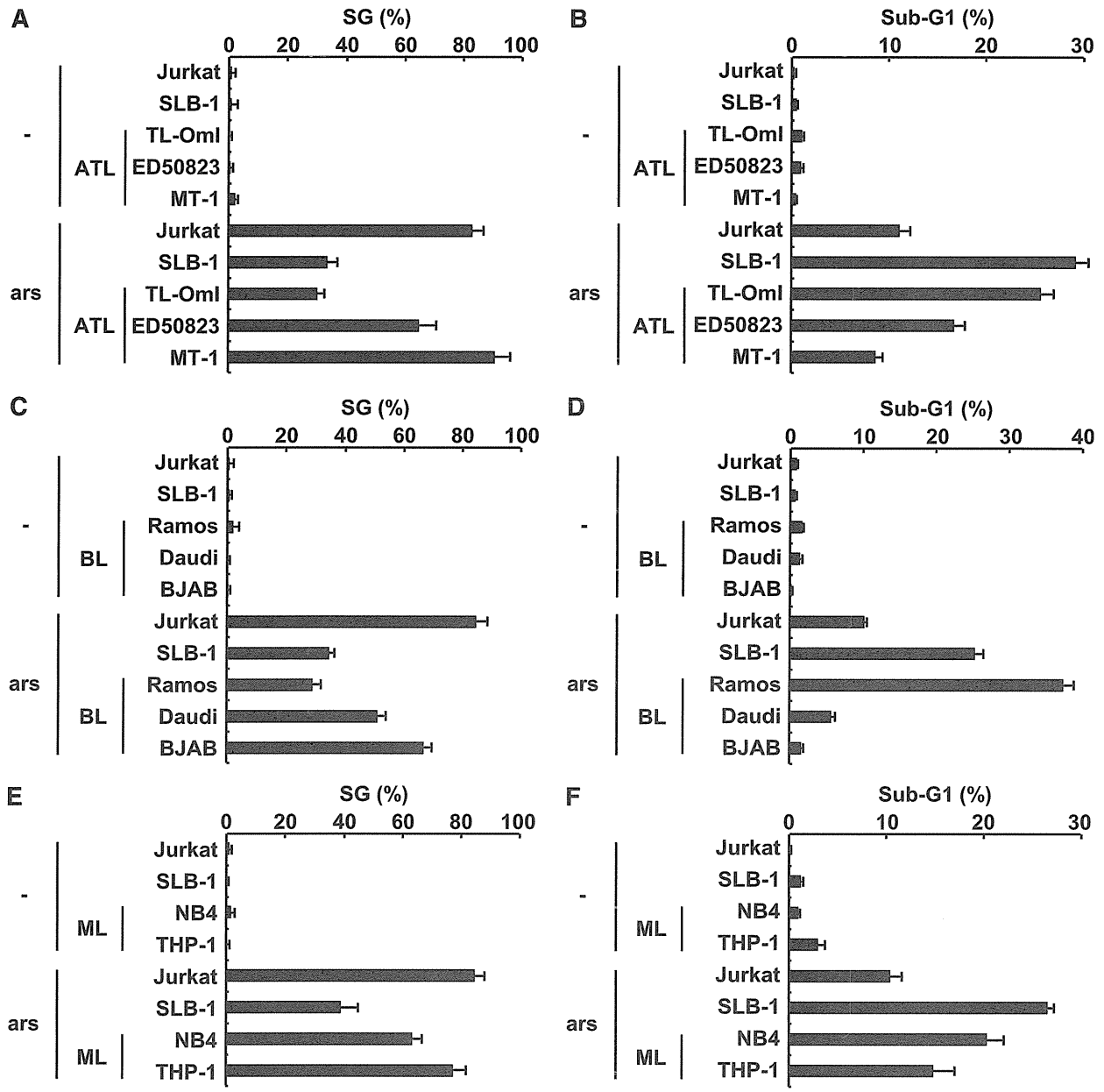

Figure 7. The level of sensitivity to arsenite-induced apoptosis in ATL, Burkitt lymphoma, and myeloid leukemia cell lines correlates with the level of SG-forming activity. (A) HTLV-1–uninfected (Jurkat), HTLV-1–infected (SLB-1; used as a positive control), and ATL-derived (TL-Oml, ED50823, and MT-1) T-cell lines were treated with 0.5 mM of sodium arsenite for 30 minutes and then were stained with anti-USP10 antibodies and Hoechst33258. The SG (%) is presented. (B) HTLV-1–uninfected (Jurkat), HTLV-1–infected (SLB-1), and ATL-derived (TL-Oml, ED50823, and MT-1) T-cell lines were treated with 5 μM of sodium arsenite for 48 hours and then were stained with PI. The proportion of the sub-G1 population (%) (apoptotic cells) was measured using flow cytometry. (C-F) The levels of arsenite-induced SG formation (%) and the proportions of the sub-G1 population (%) in the Burkitt lymphoma (C,D) and myeloid leukemia (ML) cell lines (E,F) were assessed.

by the present assay method, and such undetectable small SGs may inhibit apoptosis. We are currently studying how USP10 inhibits arsenite-induced apoptosis without visible SGs in T cells.

A clinical trial has indicated that combination therapy containing arsenic trioxide, interferon α, and zidovudine exhibits promising antileukemia activity against some forms of ATL[16]; however, it is unclear which patients are sensitive to this chemotherapy. Our present study suggests that Tax augments the sensitivity to arsenite-induced apoptosis of cells. Takeda et al showed that 66% of ATL cells exhibit inactivation of the *tax* gene because of mutation or DNA methylation.[29] Therefore, the expression of the *tax* gene in ATL cells is likely to be a factor controlling the sensitivity of ATL cells to chemotherapy containing arsenic. In addition, a single ATL-derived cell line without a Tax expression (TL-Oml) demonstrated higher sensitivity to arsenite-induced apoptosis than the other 2 ATL cell lines (Figure 7), and the different levels of arsenite sensitivity correlated with the level of SG-forming activity in the cells. Therefore, factor(s) other than Tax control(s) the sensitivity of ATL cells to arsenite-induced apoptosis, and this sensitivity might also be related to the SG-forming activity. Because the SG-forming activity is regulated by various host factors, such as G3BP1,[6] G3BP2,[43] and HDAC6,[22] these host proteins may be involved in the high arsenite-induced apoptosis of ATL cell lines without a Tax expression.

Arsenic trioxide is a highly effective chemotherapy for promyelocytic leukemia (PML).[28] Arsenic trioxide induces ROS-dependent apoptosis in several PML cell lines, including NB4, in vitro.[44,45] In our study, in addition to ATL cell lines, 5 leukemia cell lines derived from PML, myeloid leukemia, and Burkitt lymphoma exhibited distinct sensitivities to arsenite-induced apoptosis, and the level of sensitivity correlated with the degree of arsenite-induced SG formation. Therefore, understanding how USP10 and SGs control sensitivity to arsenite-induced apoptosis in hematopoietic cells will provide useful information for developing more effective chemotherapies for the treatment of hematopoietic malignancies, including ATL.

Acknowledgments

The authors thank Dr H. Miyoshi (RIKEN Tsukuba Institute, Japan) for providing the lentiviral packaging plasmids and Dr M. Masuko (Niigata University, Japan) for providing NB4 cells. The authors also thank the Takeda Pharmaceutical Company for providing recombinant human IL-2 and M. Tobimatsu for technical assistance.

This work was supported in part by a Grant-in-aid from the Ministry of Education, Culture, Sports, Science and Technology of Japan and by a Grant for the Promotion of Niigata University Research Project.

Authorship

Contribution: M.T. performed most of the experiments and contributed to the data interpretation; M.H. performed the mass spectrometry analysis and contributed to the data interpretation; G.N.M., H.M., and M.Y. assisted in conducting the experiments; Y.T. provided the anti-Tax antibody; and M.F. contributed to the conception, design, and data interpretation of the study and wrote and drafted the manuscript.

Conflict-of-interest disclosure: The authors declare no competing financial interests.

Correspondence: Masahiro Fujii, Division of Virology, Niigata University Graduate School of Medical and Dental Sciences, Niigata 951-8510, Japan; e-mail: fujiimas@med.niigata-u.ac.jp.

References

1. Anderson P, Kedersha N. RNA granules: post-transcriptional and epigenetic modulators of gene expression. *Nat Rev Mol Cell Biol.* 2009;10(6):430-436.
2. Buchan JR, Parker R. Eukaryotic stress granules: the ins and outs of translation. *Mol Cell.* 2009;36(6):932-941.
3. Takahashi M, Higuchi M, Matsuki H, et al. Stress granules inhibit apoptosis by reducing reactive oxygen species production. *Mol Cell Biol.* 2013;33(4):815-829.
4. White JP, Lloyd RE. Regulation of stress granules in virus systems. *Trends Microbiol.* 2012;20(4):175-183.
5. White JP, Cardenas AM, Marissen WE, Lloyd RE. Inhibition of cytoplasmic mRNA stress granule formation by a viral proteinase. *Cell Host Microbe.* 2007;2(5):295-305.
6. Tourrière H, Chebli K, Zekri L, et al. The RasGAP-associated endoribonuclease G3BP assembles stress granules. *J Cell Biol.* 2003;160(6):823-831.
7. Khaperskyy DA, Hatchette TF, McCormick C. Influenza A virus inhibits cytoplasmic stress granule formation. *FASEB J.* 2012;26(4):1629-1639.
8. Beckham CJ, Parker R. P bodies, stress granules, and viral life cycles. *Cell Host Microbe.* 2008;3(4):206-212.
9. Matsuoka M, Jeang KT. Human T-cell leukemia virus type 1 (HTLV-1) and leukemic transformation: viral infectivity, Tax, HBZ and therapy. *Oncogene.* 2011;30(12):1379-1389.
10. Chlichlia K, Khazaie K. HTLV-1 Tax: Linking transformation, DNA damage and apoptotic T-cell death. *Chem Biol Interact.* 2010;188(2):359-365.
11. Grassmann R, Aboud M, Jeang KT. Molecular mechanisms of cellular transformation by HTLV-1 Tax. *Oncogene.* 2005;24(39):5976-5985.
12. Boxus M, Twizere JC, Legros S, et al. The HTLV-1 Tax interactome. *Retrovirology.* 2008;5:76. doi: 10.1186/1742-4690-5-76.
13. Currer R, Van Duyne R, Jaworski E, et al. HTLV tax: a fascinating multifunctional co-regulator of viral and cellular pathways. *Front Microbiol.* 2012;3:406. doi: 10.3389/fmicb.2012.00406. Epub 2012 Nov 30.
14. Legros S, Boxus M, Gatot JS, et al. The HTLV-1 Tax protein inhibits formation of stress granules by interacting with histone deacetylase 6. *Oncogene.* 2011;30(38):4050-4062.
15. Benhar M, Engelberg D, Levitzki A. ROS, stress-activated kinases and stress signaling in cancer. *EMBO Rep.* 2002;3(5):420-425.
16. Kchour G, Tarhini M, Kooshyar MM, et al. Phase 2 study of the efficacy and safety of the combination of arsenic trioxide, interferon alpha, and zidovudine in newly diagnosed chronic adult T-cell leukemia/lymphoma (ATL). *Blood.* 2009;113(26):6528-6532.
17. Tanaka Y, Yoshida A, Tozawa H, Shida H, Nyunoya H, Shimotohno K. Production of a recombinant human T-cell leukemia virus type-I trans-activator (tax1) antigen and its utilization for generation of monoclonal antibodies against various epitopes on the tax1 antigen. *Int J Cancer.* 1991;48(4):623-630.
18. Tsubata C, Higuchi M, Takahashi M, et al. PDZ domain-binding motif of human T-cell leukemia virus type 1 Tax oncoprotein is essential for the interleukin 2 independent growth induction of a T-cell line. *Retrovirology.* 2005;2:46.
19. Higuchi M, Tsubata C, Kondo R, et al. Cooperation of NF-kappaB2/p100 activation and the PDZ domain binding motif signal in human T-cell leukemia virus type 1 (HTLV-1) Tax1 but not HTLV-2 Tax2 is crucial for interleukin-2-independent growth transformation of a T-cell line. *J Virol.* 2007;81(21):11900-11907.
20. Soncini C, Berdo I, Draetta G. Ras-GAP SH3 domain binding protein (G3BP) is a modulator of USP10, a novel human ubiquitin specific protease. *Oncogene.* 2001;20(29):3869-3879.
21. Albrecht M, Lengauer T. Survey on the PABC recognition motif PAM2. *Biochem Biophys Res Commun.* 2004;316(1):129-138.
22. Kwon S, Zhang Y, Matthias P. The deacetylase HDAC6 is a novel critical component of stress granules involved in the stress response. *Genes Dev.* 2007;21(24):3381-3394.
23. Arimoto K, Fukuda H, Imajoh-Ohmi S, Saito H, Takekawa M. Formation of stress granules inhibits apoptosis by suppressing stress-responsive MAPK pathways. *Nat Cell Biol.* 2008;10(11):1324-1332.
24. Kinjo T, Ham-Terhune J, Peloponese JM Jr, Jeang KT. Induction of reactive oxygen species by human T-cell leukemia virus type 1 tax correlates with DNA damage and expression of cellular senescence marker. *J Virol.* 2010;84(10):5431-5437.
25. Smith MR, Greene WC. Identification of HTLV-I tax trans-activator mutants exhibiting novel transcriptional phenotypes. *Genes Dev.* 1990;4(11):1875-1885.
26. Akagi T, Ono H, Nyunoya H, Shimotohno K. Characterization of peripheral blood T-lymphocytes transduced with HTLV-I Tax mutants with different trans-activating phenotypes. *Oncogene.* 1997;14(17):2071-2078.
27. Che XF, Zheng CL, Owatari S, et al. Overexpression of survivin in primary ATL cells and sodium arsenite induces apoptosis by down-regulating survivin expression in ATL cell lines. *Blood.* 2006;107(12):4880-4887.
28. Dilda PJ, Hogg PJ. Arsenical-based cancer drugs. *Cancer Treat Rev.* 2007;33(6):542-564.
29. Takeda S, Maeda M, Morikawa S, et al. Genetic and epigenetic inactivation of tax gene in adult T-cell leukemia cells. *Int J Cancer.* 2004;109(4):559-567.
30. Morgan MJ, Liu ZG. Crosstalk of reactive oxygen species and NF-κB signaling. *Cell Res.* 2011;21(1):103-115.
31. Anrather J, Racchumi G, Iadecola C. NF-kappaB regulates phagocytic NADPH oxidase by inducing the expression of gp91phox. *J Biol Chem.* 2006;281(9):5657-5667.
32. Suzuki T, Ohsugi Y, Uchida-Toita M, Akiyama T, Yoshida M. Tax oncoprotein of HTLV-1 binds to the human homologue of Drosophila discs large tumor suppressor protein, hDLG, and perturbs its function in cell growth control. *Oncogene.* 1999;18(44):5967-5972.
33. Arpin-André C, Mesnard JM. The PDZ domain-binding motif of the human T cell leukemia virus type 1 tax protein induces mislocalization of the tumor suppressor hScrib in T cells. *J Biol Chem.* 2007;282(45):33132-33141.
34. Okajima M, Takahashi M, Higuchi M, et al. Human T-cell leukemia virus type 1 Tax induces an aberrant clustering of the tumor suppressor Scribble through the PDZ domain-binding motif

dependent and independent interaction. *Virus Genes.* 2008;37(2):231-240.

35. Makokha GN, Takahashi M, Higuchi M, Saito S, Tanaka Y, Fujii M. Human T-cell leukemia virus type 1 Tax protein interacts with and mislocalizes the PDZ domain protein MAGI-1. *Cancer Sci.* 2013;104(3):313-320.
36. Harris BZ, Lim WA. Mechanism and role of PDZ domains in signaling complex assembly. *J Cell Sci.* 2001;114(Pt 18):3219-3231.
37. Subbaiah VK, Kranjec C, Thomas M, Banks L. PDZ domains: the building blocks regulating tumorigenesis. *Biochem J.* 2011;439(2):195-205.
38. Peloponese JM Jr, Iha H, Yedavalli VR, et al. Ubiquitination of human T-cell leukemia virus type 1 tax modulates its activity. *J Virol.* 2004;78(21): 11686-11695.
39. Nasr R, Chiari E, El-Sabban M, et al. Tax ubiquitylation and sumoylation control critical cytoplasmic and nuclear steps of NF-kappaB activation. *Blood.* 2006;107(10): 4021-4029.
40. Yasunaga J, Lin FC, Lu X, Jeang KT. Ubiquitin-specific peptidase 20 targets TRAF6 and human T cell leukemia virus type 1 tax to negatively regulate NF-kappaB signaling. *J Virol.* 2011; 85(13):6212-6219.
41. Lavorgna A, Harhaj EW. An RNA interference screen identifies the Deubiquitinase STAMBPL1 as a critical regulator of human T-cell leukemia virus type 1 tax nuclear export and NF-κB activation. *J Virol.* 2012;86(6):3357-3369.
42. Fryrear KA, Guo X, Kerscher O, Semmes OJ. The Sumo-targeted ubiquitin ligase RNF4 regulates the localization and function of the HTLV-1 oncoprotein Tax. *Blood.* 2012;119(5): 1173-1181.
43. Matsuki H, Takahashi M, Higuchi M, Makokha GN, Oie M, Fujii M. Both G3BP1 and G3BP2 contribute to stress granule formation. *Genes Cells.* 2013;18(2):135-146.
44. Chen GQ, Zhu J, Shi XG, et al. In vitro studies on cellular and molecular mechanisms of arsenic trioxide (As2O3) in the treatment of acute promyelocytic leukemia: As2O3 induces NB4 cell apoptosis with downregulation of Bcl-2 expression and modulation of PML-RAR alpha/PML proteins. *Blood.* 1996;88(3):1052-1061.
45. Jing Y, Dai J, Chalmers-Redman RM, Tatton WG, Waxman S. Arsenic trioxide selectively induces acute promyelocytic leukemia cell apoptosis via a hydrogen peroxide-dependent pathway. *Blood.* 1999;94(6):2102-2111.

Kinpara et al. Retrovirology 2013, 10:52
http://www.retrovirology.com/content/10/1/52

RETROVIROLOGY

RESEARCH Open Access

Interferon-α (IFN-α) suppresses HTLV-1 gene expression and cell cycling, while IFN-α combined with zidovudin induces p53 signaling and apoptosis in HTLV-1-infected cells

Shuichi Kinpara[1,2], Mami Kijiyama[1], Ayako Takamori[1], Atsuhiko Hasegawa[1], Amane Sasada[1], Takao Masuda[1], Yuetsu Tanaka[3], Atae Utsunomiya[4] and Mari Kannagi[1*]

Abstract

Background: Human T-cell leukemia virus type-1 (HTLV-1) is the causative retrovirus of adult T-cell leukemia/lymphoma (ATL) and HTLV-1-associated myelopathy/tropical spastic paraparesis (HAM/TSP). HTLV-1 gene expression is maintained at low levels *in vivo* by unknown mechanisms. A combination therapy of interferon-α (IFN-α) and zidovudin (AZT) shows therapeutic effects in ATL patients, although its mechanism is also obscure. We previously found that viral gene expression in IL-2-dependent HTLV-1-infected T-cells (ILTs) derived from ATL patients was markedly suppressed by stromal cells through a type I IFN response. Here, we investigated the effects of IFN-α with or without AZT on viral gene expression and cell growth in ILTs.

Results: ILTs expressed variable but lower amounts of HTLV-1 Tax protein than HTLV-1-transformed HUT102 cells. Following the addition of IFN-α, the amounts of HTLV-1 p19 in the supernatants of these cells decreased in three days, while HTLV-1 gene expression decreased only in ILTs but not HUT102 cells. IFN-α also suppressed the spontaneous HTLV-1 induction in primary ATL cells cultured for 24 h. A time course study using ILTs revealed that the levels of intracellular Tax proteins decreased in the first 24 h after addition of IFN-α, before the reduction in HTLV-1 mRNA levels. The initial decreases of Tax protein following IFN-α treatment were observed in 6 of 7 ILT lines tested, although the reduction rates varied among ILT lines. An RNA-dependent protein kinase (PKR)-inhibitor reversed IFN-mediated suppression of Tax in ILTs. IFN-α also induced cell cycle arrest at the G0/G1 phase and suppressed NF-κB activities in these cells. AZT alone did not affect HTLV-1 gene expression, cell viability or NF-κB activities. AZT combined with IFN-α markedly induced cell apoptosis associated with phosphorylation of p53 and induction of p53-responsive genes in ILTs.

Conclusions: IFN-α suppressed HTLV-1 gene expression at least through a PKR-mediated mechanism, and also induced cell cycle arrest in ILTs. In combination with AZT, IFN-α further induced p53 signaling and cell apoptosis in these cells. These findings suggest that HTLV-1-infected cells at an IL-2-dependent stage retain susceptibility to type I IFN-mediated regulation of viral expression, and partly explain how AZT/IFN-α produces therapeutic effects in ATL.

Keywords: ATL, HTLV-1, IFN-α, PKR, Innate immunity, Anti-viral therapy, AZT, p53

* Correspondence: kann.impt@tmd.ac.jp
[1]Department of Immunotherapeutics, Graduate School of Medical and Dental Sciences, Tokyo Medical and Dental University, 1-5-45 Yushima, Bunkyo-ku, Tokyo 113-8519, Japan
Full list of author information is available at the end of the article

Background

Human T-cell leukemia virus type 1 (HTLV-1) causes adult T-cell leukemia/lymphoma (ATL) [1-3], a malignant lympho-proliferative disorder resistant to chemotherapy. The virus is also responsible for HTLV-1-associated myelopathy/tropical spastic paraparesis (HAM/TSP) [4,5], a chronic inflammatory demyelinating disorder. Despite such severe clinical outcomes, levels of HTLV-1 gene expression are thought to be very low *in vivo*. HTLV-1 mRNA, but not proteins, are detectable in peripheral blood mononuclear cells (PBMCs) of HTLV-1-infected individuals [6]. Although undetectable, a low level of HTLV-1 proteins must be present *in vivo*, as HTLV-1-infected individuals maintain antibodies against HTLV-1 structural proteins and Tax protein-specific cytotoxic T lymphocytes.

Recent therapeutic approaches, such as allogeneic hematopoietic stem cell transplantation (allo-HSCT) [7,8], a humanized antibody therapy targeting CCR4 [9,10], or anti-viral therapy with interferon (IFN)-α and zidovudin (AZT) [11-13] partly improved ATL prognosis. *Ex vivo* studies have indicated that graft-versus-tumor responses including anti-Tax cytotoxic T-cells were potentially involved in the therapeutic mechanisms of allo-HSCT [14], and that the CCR4-antibodies were capable of inducing antibody-dependent cellular cytotoxicities [15]. However, combining AZT/IFN-α hardly affects HTLV-1-infected cells *in vitro* [16], and the mechanisms of its therapeutic effects remain unclear. A recent report indicated that the triple combination of arsenic trioxide/IFN-α/AZT demonstrated more favorable therapeutic effects in ATL patients [17]. The combination of arsenic trioxide and IFN-α has been reported to induce proteolysis of Tax in HTLV-1-infected cells *in vitro* [18,19]. As IFN-α is indispensable in AZT/IFN-α, arsenic trioxide/IFN-α or arsenic trioxide/IFN-α/AZT therapies, ATL cells might be susceptible to IFNs *in vivo*.

It is well established that HTLV-1-infected cells are resistant to type I IFNs *in vitro*. For example, IFN-α reduced the virus release but not viral protein synthesis in HTLV-1-transformed HUT102 or MT-2 cells [20]. The mechanisms of the resistance to type I IFNs in HTLV-1-infected cells include reduction in the phosphorylation of Tyk2 and STAT2 [21], Tax-mediated competition with CREB binding protein/p300 [22], Tax-mediated up-regulation of SOCS1 [23,24], and up-regulation of IRF4 [25], all of which result in inhibition of IFN signaling. This may explain why IFN-α combined with AZT does not affect HTLV-1-infected cells *in vitro*, while conflicting with the clinical effects of AZT/IFN-α therapy in ATL patients. This discrepancy between *in vivo* and *in vitro* systems can be partially attributed to differences in status of HTLV-1-infected cells between the two systems.

We previously found that HTLV-1-infected cells could induce type I IFN responses in co-cultured stromal cells [26]. We also found that viral expression in HTLV-1-infected T-cells is markedly suppressed at both mRNA and protein levels through type I IFN responses mediated by stromal cells co-cultured [26]. This observation again conflicts with the previous notion of HTLV-1-mediated resistance to type I IFNs *in vitro*. Our experimental system differed from previous studies in two ways. First, we used IL-2-dependent HTLV-1-infected T-cells (ILTs) derived from ATL patients, while previous studies used IL-2-independent HTLV-1-transformed cell lines such as HUT102. Second, we used stromal cells as effectors; these mediated the type I IFN response, but could have also produced multiple factors other than IFNs.

In the present study, we investigated whether purified type I-IFNs can affect viral expression and cell growth of HTLV-1-infected cells by using various ILTs. Here we report a novel finding that IFN-α suppresses intracellular Tax expression at a translational level at least through PKR. We further demonstrate that IFN-α activates p53 pathways in cooperation with AZT, partly explaining the mechanisms of the therapeutic effects of AZT/IFN-α in ATL.

Results

Effects of IFN-α on HTLV-1 p19 release and viral transcription

We evaluated the baseline levels of HTLV-1 gene expression in HUT102, ILT-Hod and ILT-#29 cell lines (Figure 1A). Relative levels of HTLV-1 mRNA in ILT-Hod and ILT-#29 cells were comparable with those in HUT102 cells. However, the levels of Tax protein in ILT-Hod and ILT-#29 cells were much lower than those of HUT102, and were barely detectable by immunoblotting only after stimulation of ILTs with phorbol 12-myristate 13-acetate (PMA). Flow cytometry results also indicated that ILT-Hod and ILT-#29 cells expressed smaller amounts of intracellular Tax protein than HUT102 cells. In addition, our analyses often identified Tax-negative cell populations in ILTs, with the ratio of these populations fluctuating during culture. These cells are also HTLV-1-infected, as all the cells in ILT-Hod and ILT-#29 cultures express HTLV-1 Gag protein after stimulation with PMA (Figure 1A insert), suggesting a dynamic turnover of HTLV-1 proteins in ILTs. Tax expression in HUT102 cells was apparently stable (Figure 1A).

We added IFN-α at various concentrations (300, 3000, and 30000 IU/ml) on HUT102, ILT-Hod, and ILT-#29 cells (Figure 1B). The amounts of HTLV-1 p19 released in supernatants significantly decreased after 72 h in culture for all the cell lines tested. Gag mRNA levels were also decreased in ILT-Hod and ILT-#29 in 3 days of culture (Figure 1B). These suppressive effects were observed at all doses of IFN-α used, indicating that 300 IU/ml of IFN-α was sufficient to produce these effects.